

**EXPERIMENTAL INVESTIGATION OF
QUALITY CHARACTERISTICS DURING
ABRASIVE WATER JET MACHINING ON
BOROSILICATE GLASS**

A Thesis Submitted in Partial Fulfilment of the Requirements for
Awarding the Degree of

**MASTER OF MECHANICAL ENGINEERING
FACULTY OF ENGINEERING AND TECHNOLOGY**

Submitted by

PIYUSH KUMAR

Registration No. - 160290

Examination Roll No. - M4MEC23004

Under the guidance of

SUMAN NIHAR

Dr. RANJIB BISWAS

Dr. JISNU BASU

**DEPARTMENT OF MECHANICAL ENGINEERING
JADAVPUR UNIVERSITY
KOLKATA-700032**

INDIA

2023

**FACULTY OF ENGINEERING AND TECHNOLOGY
JADAVPUR UNIVERSITY**

CERTIFICATE OF RECOMMENDATION

This is to certify that **Mr. Piyush Kumar** has completed his thesis entitled “**Experimental investigation of quality characteristics during abrasive water jet machining on borosilicate glass**”, under the supervision and guidance of **Suman Nihar and Dr. Rajib Biswas**, Jadavpur University, Kolkata and **Dr. Jisnu Basu**, Saha Institute of Nuclear Physics, Kolkata. We are satisfied with his work, which is being presented for the partial fulfilment of the degree of **Master of Mechanical Engineering**, Jadavpur University, Kolkata-700032.



THESIS SUPERVISOR

Suman Nihar

Assistant Professor

Dept. of Mechanical Engineering

Jadavpur University

Kolkata-700032

THESIS CO-SUPERVISOR

Dr. Ranjib Biswas

Associate Professor

Dept. of Mechanical Engineering

Jadavpur University

Kolkata-700032

THESIS CO-SUPERVISOR

Dr. Jisnu Basu

Saha Institute of Nuclear Physics

Kolkata-700064

Dr. Amit Karmakar

HEAD

Dept. of Mechanical Engineering

Jadavpur University

Kolkata-700032

Dr. Ardhendu Ghosal

DEAN

Faculty of Engineering and Technology

Jadavpur University

Kolkata-700032

**FACULTY OF ENGINEERING AND TECHNOLOGY
JADAVPUR UNIVERSITY
KOLKATA**

CERTIFICATE OF APPROVAL*

The foregoing thesis is hereby approved as a creditable study of an engineering subject carried out and presented in a manner of satisfactory to warrant its acceptance as a pre-requisite to the degree for which it has been submitted. It is understood that by this approval, the undersigned do not necessarily endorse or approve any statement made, opinion expressed and conclusion drawn therein but thesis only for the purpose for which it has been submitted.

Committee of final examination for evaluation of thesis:

Signature of Examiners

* Only in case the thesis is approved.

ACKNOWLEDGEMENT

First and foremost, I'd like to convey my sincere admiration and appreciation to my advisor and mentor, **Suman Nihar, Dr. Ranjib Biswas and Dr. Jisnu Basu** who has been the driving force behind this work. I owe him a huge debt of gratitude for his unwavering support, invaluable advice, and for pulling me forward in every aspect of my academic career. His presence and excitement have had a significant impact on my work and vision for the future. I consider it a blessing to be able to work with such a wonderful person.

I'd also like to take this opportunity to thank all of the faculty members in the Mechanical Engineering department for their mental support, invaluable assistance, and cooperation throughout the course of this thesis work.

My sincere gratitude goes out to my friends and classmates for their invaluable assistance, cooperation, and support. I have enjoyed their companionship so much during my stay at Jadavpur University, Kolkata.

I am especially indebted to my parents, Mr. Krishna Kumar Singh and Mrs. Manju Singh for their love, sacrifice, and support towards my education. I would like to thank my brother Pratyush for his friendly support at various stages of the project work.

Name - Piyush Kumar
Registration No. - 160290
Examination Roll No. - M4MEC23004

ABSTRACT

Abrasive water jet machining process (AWJM) is a modern machining technique that is excellent for cutting materials of all hardness, from Inconel to rubber. Abrasive water jet machining has drawn greater focus from researchers because of its extensive operations and exceptional finish obtained during the machining process.

The framed study addresses machining parameters effect on material removal rate (MRR) and radius of curvature (Rc) of borosilicate glass during cutting by AWJM. For the trials, four different levels of each of the machining parameters namely, - water pressure, abrasive mass flow rate, traverse speed and standoff distance - have been selected. Experiments have been conducted using response surface methodology (RSM) and investigated how machining parameters affect material removal rate and radius of curvature.

Significance of the machining parameters on material removal rate and radius of curvature have been found using analysis of variance (ANOVA). Observations have been taken on the most significant input parameters affecting the variations of MRR and radius of curvature. Single-objective optimization and multi-objective optimization have been performed and compared together with desirability function approach (DFA). At last, confirmation test has been performed to validate the obtained result.

Table of contents

Chapter	Page No.
ABSTRACT	V
LIST OF FIGURES	IX
LIST OF TABLES	XI
LIST OF NOMENCLATURES	XII
Chapter 1: Introduction	1-12
1.1 Overview	1
1.2 Abrasive water jet machining	2-12
1.2.1 Introduction to Abrasive Water Jet Machining	2-3
1.2.2 Principle	3-4
1.2.3 Material removal mechanism	4-5
1.2.4 Working	6-7
1.2.5 Process parameters	8-9
1.2.6 Cause-Effect diagram	9
1.2.7 Applications	9-11
1.2.8 Advantages	11-12
1.2.9 Limitations	12
Chapter 2: Literature review and research objectives	13-19
2.1 Literature review	13-18
2.2 Research objective	18-19
Chapter 3: Experimental Setup	20-24
3.1 AWJM system	20-24
3.1.1 AWJ Machine specifications	20
3.1.2 Equipments	20-24
3.1.2.1 Intensifier Pump	21
3.1.1.2 Abrasive Feed System	21-23
3.1.1.3 Water jet cutting head	23
3.1.1.4 Position control system	23

3.1.1.5 Catcher Unit	23-24
3.2 Flow chart of experiment	24
Chapter 4: Design of experiment and Optimization technique	25-31
4.1 History of Design of Experiment (DOE)	26-27
4.2 Uses of DOE	27-28
4.3 RSM approach to DOE	28-30
4.4 Analysis of variance (ANOVA)	30
4.5 Optimization Techniques	31
4.5.1 Desirability function approach (DFA)	31
Chapter 5: Experimental plan and procedures	32-39
5.1 Experimental Plan	32
5.2 Work material	32-33
5.2.1 Specimen	32-33
5.2.2 Abrasive particles	33
5.3. Experimental Details	33-36
5.3.1. Selection of process parameters	33
5.3.2. Finding the limits of process parameters	34
5.3.3. Experimental design	34-36
5.4 Experimental Procedure	37
5.5 Testing Equipments	38-39
5.5.1 Scanning electron microscope	38-39
5.5.2 Weighing machine	39
Chapter 6: Experimental Investigation and Optimization	40-58
6.1 Experimental Results	40
6.2 Development of mathematical models using RSM	40-44
6.2.1 Analysis of material removal rate (MRR)	42
6.2.2 Analysis of radius of curvature (Rc)	42-44
6.3 Process parameters effects on outputs	45-54
6.3.1 Effects of process parameters on material removal rate	45-49

6.3.2 Effects of process parameters on radius of curvature	50-54
6.4 Optimization of process parameters	54-57
6.4.1 Single-objective optimization	54-56
6.4.2 Multi - objective optimization	56-57
6.5 Confirmation test	58
Chapter 7: Conclusion	59-60
7.1 Conclusion	59-60
7.2 Future scope of work	60
References	61-68

LIST OF FIGURES

Figure No.		Page No.
 <u>Chapter 1</u>		
Fig. 1.1	Erosion process on different materials	5
Fig. 1.2	Various terms of the AWJ machined surface	5
Fig. 1.3	Working principle of AWJM	7
Fig. 1.4	Cause-Effect diagram	10
 <u>Chapter 3</u>		
Fig. 3.1	Complete setup of abrasive water jet machine	22
Fig. 3.2	Flow chart of experiment	24
 <u>Chapter 4</u>		
Fig. 4.1	Central composite design	30
 <u>Chapter 5</u>		
Fig. 5.1	Machined borosilicate glass	37
Fig. 5.2	Striation marks on cut surface	39
 <u>Chapter 6</u>		
Fig. 6.1	Response surface of MRR with AFR and TS	45
Fig. 6.2	Response surface of MRR with WP and SOD	46
Fig. 6.3	Response surface of MRR with TS and SOD	47
Fig. 6.4	Response surface of MRR with AFR and SOD	48
Fig. 6.5	Response surface of MRR with TS and WP	49
Fig. 6.6	Response surface of MRR with WP and AFR	49
Fig. 6.7	Response surface of Rc with WP and AFR	50
Fig. 6.8	Response surface of Rc with TS and SOD	51
Fig. 6.9	Response surface of Rc with AFR and TS	52
Fig. 6.10	Response surface of Rc with WP and SOD	52
Fig. 6.11	Response surface of Rc with SOD and AFR	53

Fig. 6.12	Response surface of Rc with WP and AFR	54
Fig. 6.13	Optimization result for material removal rate	55
Fig. 6.14	Optimization result for radius of curvature	56
Fig. 6.15	Multi-objective optimization results	57

LIST OF TABLES

Table No.		Page No.
<u>Chapter 3</u>		
Table 3.1	Details of the machine	21
<u>Chapter 5</u>		
Table 5.1	Mechanical Properties of borosilicate glass	33
Table 5.2	Physical and chemical properties of garnet	33
Table 5.3	Parameters with notations, units and levels	34
Table 5.4	Coded Design Matrix	35
Table 5.5	Uncoded Design Matrix	36
<u>Chapter 6</u>		
Table 6.1	Design matrix and measured experimental results	41
Table 6.2	Analysis of variance for MRR	43
Table 6.3	Analysis of variance for Rc	44
Table 6.4	Final verification experiment	58

LIST OF ABBREVIATIONS

AFR	Abrasive Flow Rate
AMF	Abrasive flow mass
ANOVA	Analysis of Variance
AWJ	Abrasive water jet
AWJM	Abrasive Water Jet Machining
CCD	Central composite design
ChM	Chemical Machining
EBM	Electron Beam Machining
ECM	Electrochemical Machining
EDM	Electric Discharge machining
DFA	Desirability function approach
DOE	Design of experiment
DOC	Depth of cut
HAZ	Heat affected zone
LBM	Laser Beam Machining
MOO	Multi-objective optimization
MRR	Material Removal Rate
PAM	Plasma Arc Machining
Ra	Surface roughness
Rc	Radius of curvature
RSM	Response surface methodology
SEM	Scanning Electron Microscope
SOD	Stand-off distance
SOO	Single objective optimization
TS	Traverse speed
TWR	Tool wear rate
USM	Ultrasonic Machining
WP	Water pressure

CHAPTER 1

INTRODUCTION

1.1 Overview

Humans, since their birth tend to evolve and make their surroundings a better place to live. In process to evolve they tend to invent things which make their way of living easier and also upgrade the same with time. So, how could the manufacturing industry remain untouched? New developments are taking place to process new materials at very faster rate in present situation. The manufacturing industries are relying on the modern manufacturing process which maybe conventional or non-conventional in nature. Due to the increase in the demand of processing of hard and brittle materials, modern manufacturing has led to the growth of latest non-conventional manufacturing methods. People are showing high interest in the development of special materials which are difficult to process using existing technology, for quite a few years now. The unique properties of such materials can be high strength, high specific stiffness, high heat resistant, high hardness and resistant to corrosion, etc. One can face a lot of technical difficulties and economic burden in processing such materials using conventional methods. As a result, development of non-conventional machining processes took place. Now, a question arises here what we will do after processing such materials? So, one can easily find the usage of such materials in aerospace, automobile and space applications, etc.

These non-conventional processes can be labelled as mechanical, electrical, thermal and chemical methods based on the type of energy we are using to get our end results. To name a few, we have Ultrasonic Machining (USM), Abrasive Jet Machining (AJM), Abrasive Water Jet Machining (AWJM), Electric Discharge machining (EDM), Electrochemical Machining (ECM), Chemical Machining (ChM), Electron Beam Machining (EBM), Laser Beam Machining (LBM) and Plasma Arc Machining (PAM).

1.2 Abrasive Water Jet Machining

1.2.1 Introduction to AWJM

Technology breakthroughs in the domains of engineering and technology have helped with this, since we are trying to do transition to more effective methods as a result of the worrisome rate at which our resources are depleting in the world, we live in. Currently, we are switching from conventional to non-conventional energy sources for the creation of new technologies and procedures. There is a need to exploit unconventional energy sources and unconventional manufacturing methods over conventional ones like welding and casting etc. [1]. Furthermore, the conventional techniques pollute the environment by producing tiny chips, fibres, and dust particles. Consequently, there is a need for the processes that are not only effective but also environmentally benign [2, 3]. In addition, traditional machining causes extra tool wear, high cutting pressure, inadequate dimensional accuracy, poor surface finish, etc. [4, 5]. This necessitates the use of non-traditional machining techniques. Among a variety of non-conventional machining techniques like Electro-chemical machining (ECM), Electro discharge machining (EDM), Ultrasonic machining (USM), Abrasive Water Jet machining (AWJM), is used for cutting hard and brittle materials. The AWJM have been chosen in this research work as this machining has higher material removal rate (MRR), relatively no tool wear rate (TWR) and nearly no heat affected zone (HAZ) [6]. Abrasive water jet machining frameworks are now widely used for different mechanical and machining applications because of the ability they have to cut a wide range of metals and non-metals, for example, aluminium, treated steel, cast iron, titanium and its compounds, fibre-strengthened composites, high carbon steels, and so on [7]. Construction, automotive engineering, aviation, maritime engineering and fabrication of a wide range of industrial items all make use of AWJ machining. The recognition of abrasive water jet machines is growing these days for comprehensive cutting and having applications in the design of offices and residences, etc. [8, 9].

The fundamental idea of AWJM is that the material removal mechanism in the process is by shearing and tearing [10]. It employs an intense stream of water at about

200 m/s impinging on the work piece through a nozzle while keeping a stand-off distance between the nozzle and the work piece so that unwanted materials get removed due to the kinetic energy of the abrasive particles acquired by the rapid travel of the water jet [6]. Pumps are used to raise the pressure up to 400 MPa while drawing water from the tank. The accumulator temporarily holds water under pressure and supplies it without pressure fluctuations when needed for processing. The water is under pressure as it travels through tiny nozzles, where the potential energy from the pressure is transformed into kinetic energy and a speed of about 1000 m/s is produced. The abrasive particles are introduced into the mixing chamber by very high velocity water jet. To perform the cutting operation on the sample that is being hit by this jet, a mixed jet of water and abrasive particles is sent in this direction. The catcher also gathers the abrasive particles and water that are fed to the tank and hopper. The most often employed abrasive particles in the AWJM are garnet and aluminium oxide. In addition to these, sand and glass globules are used as well [11, 12]. Apart from enhanced machining flexibility, this machining technique also has quick cutting rates, low cutting pressure, multidirectional cutting capability and almost no thermal deformation. However, it has some drawbacks, most notably are the potential for noise and vibration [13].

1.2.2 Principle

Abrasive water jet machining is a process in which a very high speed water jet mixed with abrasive particles is used to cut a variety of materials. Abrasive water jet machining is an advanced form of water jet machining wherein the water jet is injected with abrasive particles like garnet, silicon carbide, or aluminium oxide in order to increase the rate of material removal. Abrasive water jet machining process can be employed to a variety of materials ranging from soft like rubber and foam to hard and brittle ones like metal, ceramics, and glass. The cutting streams that are controlled by computers mostly, is responsible for making the cutting process to be more efficient and accurate.

The AWJM procedure is suited for cutting materials that are challenging to cut using thermal cutting or laser cutting. The AWJM machines discharge a highly concentrated, supersonic spray of water at the material in order to smoothly erode

materials without producing any heat. As a result, all thermal and mechanical deformation brought on by traditional cutting techniques are completely eliminated by the AWJM process. Furthermore, slanted cuts are possible since the water jet nozzle can be targeted at the material at any angle. Pure water free of any abrasives is used to cut soft items like food and linens.

1.2.3 Material removal mechanism

The term "erosion" refers to the sort of wear which results from the constant impact of abrasive particles. In the process of removing material using AWJ machining, the effect of the abrasive particles is fundamental. Abrasive particles remove material from the surface of the work piece by employing four distinct mechanisms, namely cutting, fatigue, melting, and brittle fracture [14]. Two primary forms of material removal occur in AWJ as a result of micro cutting, encompassing cutting and deformation erosive wear mechanism [15].

Ploughing deformation is considerable for spherical abrasive particles [16] as seen in Fig. 1.1(a), whereas cutting deformation occurs through sharp-edged angular particles. The combined action of cutting wear and deformation wear mechanisms cause ductile erosion. The target material is typically impinged by the abrasive particles at a low angle of incidence in the cutting wear zone, creating a smooth cutting zone. The cutting zone develops a rough surface with striation lines under deformation wear as seen in Fig. 1.1(b), which happens at a steep angle of attack [17, 18]. Material removal during the brittle erosion process takes place through the propagation of cracks and chipping as a consequence of contact stresses brought on by the impact of abrasive particles [19]. The material removal mechanism in the workpiece is affected by jet impact angles. Oblique jet impact angle was associated with a highly effective ductile shearing action that limited the appearance of fracture traces and insufficient chip removal on the machined workpiece surface [20, 21].

Three zones have been identified on the AWJ surface, Fig. 2.1 provides specifics. The expansion of the jet prior to impingement and the variation in jet energy with radial distance provide the initial damage region at the top kerf wall cut surface. The abrasive impingement angle in this area is far more than what must be achieved for

the remaining depth of cut. Under the first damage region, the cutting region known for smoothness and the cutting region known for roughness coexist. They can be identified by waviness profiles. The machined surface implements the abrasive particle size in the region of the smooth cutting. On the contrary, the surface characteristics of the rough cutting region are controlled by cutting parameters that affect jet kinetic energy.

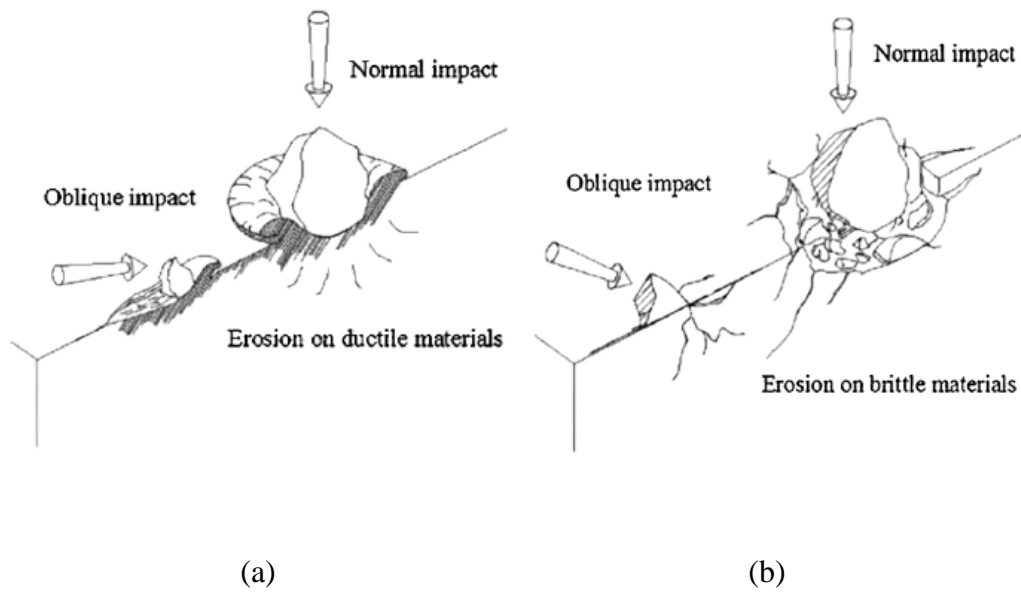


Fig. 1.1: Erosion process on (a) ductile materials (b) brittle materials [60].

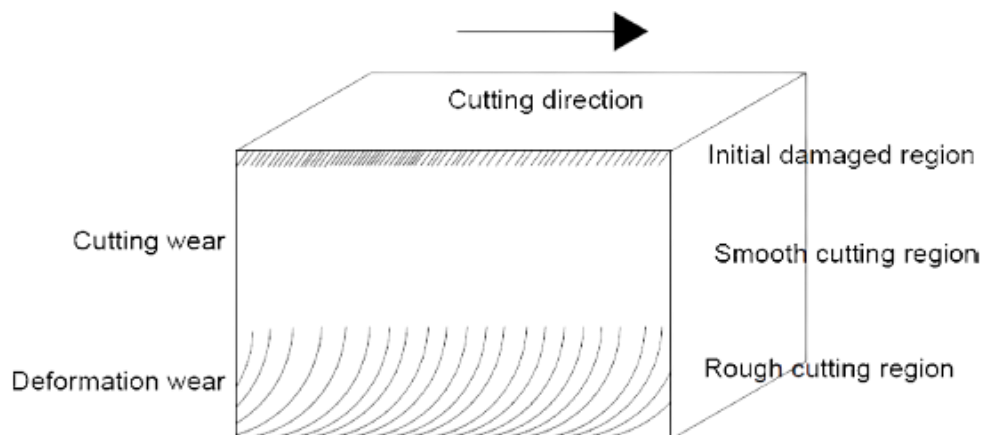


Fig. 1.2: Various terms of the AWJ machined surface [60].

1.2.4 Working

The aforementioned manufacturing technique is based on the principle of mechanical erosion in which acceleration of abrasive particles through a high pressure jet is used to cut the material on which machining is being done. Thus as a result high kinetic energy is produced due to high velocity which leads to erosion of the workpiece rapidly. Due to an increase in the water pressure, there is a rise in kinetic energy of water jet mixture which leads to the increment in the momentum that gets transferred to the abrasive particles. Consequently, the target material is cut as a result of the abrasive particles changed momentum. It is feasible to cut a variety of materials, including metals, composites, ceramics, and rocks, with the high velocity abrasive water jet. Material gets removed by erosion wear on the upper surface, which is then followed by wear deformation at the lower regions of the workpiece being cut.

The abrasive water jet system works on the basis that water is raised to a high pressure by a high-pressure system and then delivered throughout the system. An intensifier pump, powered by hydraulic oil that has been pressurised and delivered to a hydraulic radial displacement pump to create a carrier medium for the abrasive material. The water supply system is used for transporting water from the pump at high pressure to the cutting head. The system's main components are high-pressure pipes and various types of valves and joints in supplying water.

The abrasive feed system is used for mixing water and the abrasive particles. The abrasive feed system consists of an abrasive hopper, a delivery hose and a metering valve. Abrasive particles are carried to the abrasive inlet on the nozzle assembly from the metering valve via the delivery hose. To control the abrasive mass flow rate, there is an ON/OFF switch. Abrasives are stored in the container known as hopper. It is important that the distance between the hopper and the nozzle assembly should be minimal in order to get maximum cutting efficiency.

The nozzle assembly also called as the cutting head is comprised of a mixing chamber, an orifice and an abrasive water jet nozzle. The cutting head is responsible for providing and controlling the high-pressure water jet. It comprises of diameter which ranges from 1 to 5 mm and the orifice is used to transform the high pressure

water into high velocity water jet. The most commonly used materials for orifice are diamond and sapphire. The mixing chamber is placed in between the nozzle and orifice where mixing of water and abrasive particles sucked through vacuum took place. Successively acceleration of abrasive particles through nozzle took place after mixing. The commonly used material for the nozzle is tungsten carbide. In order to get the optimal cutting performance is via nozzle length and diameter. The nozzle diameter is estimated to be 2.5 – 5 times the size of the diameter of the orifice. It is important to note here that the nozzle length must be accurate because a shorter one can restrict the assurance of desired acceleration of the abrasive particles, on the other hand a longer one can lead to excessive wear of nozzle owing to impact of abrasive particles, which results in loss of momentum as well.

Abrasive water jet machining is used to remove material from targeted workpiece by the principle of mechanical erosion. The aforementioned principle is based on the abrasive particles being mixed with a high velocity stream of water jet to target the material of interest. The high kinetic energy gets converted into the pressure energy creating high stress on the work piece and thus resulting in removal of material from the workpiece.

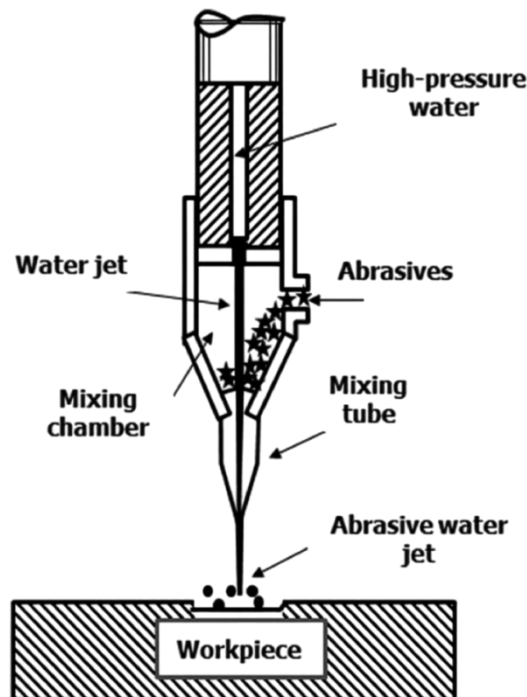


Fig. 1.3: Working principle of AWJM [61].

1.2.5 Process parameters

A number of process parameters decides the quality of the part in AWJM that need to be properly controlled. Some of the important parameters are discussed below:

- **Abrasive Type:** The type of abrasive used is the most important parameter in the process of abrasive water jet machining as it is responsible for the material removal rate and the machining accuracy. When it comes to choose the abrasive type, hardness becomes the basis of selection. Rate of material removal and accuracy of machining are critical for selection of abrasive type as well. Some of the most widely used abrasive types in the abrasive water jet machining process are glass beads, garnet, aluminium oxide, silica, silicon carbide, crushed glass, glass beads, and sodium bicarbonate.
- **Abrasive Grain Size:** There is a vital role of abrasive grain size in AWJM process. Fine particles are used for polishing and finishing operations in general, whereas the coarse grain particles are commonly used for the cutting processes. Abrasives with greater size and much less particles per unit weight have smaller mess number.
- **Water Jet Pressure:** In AWJM, the flow of the abrasive is reliant on the water jet pressure in order to cut the workpiece. With an increase in water pressure, kinetic energy of abrasive particles tends to rise, increasing their capacity to remove material while reducing surface roughness and shortening the process overall duration. Higher water pressure increases particle velocity and fragmentation within the abrasive nozzle, which improves surface quality. However, if the water pressure is too great, it could have a detrimental effect on the material. Abrasive particles lose their power to cut when they are too fractured under extreme water pressure.
- **Standoff Distance:** One other important parameter in abrasive water jet machining process is the stand-off distance (SOD). The SOD is that distance which covers the distance from the work surface to the tip of the nozzle. As the SOD increases, the jet has a greater chance to expand before impacting the work surface. With a larger SOD, the cutting process produces a greater jet diameter, which reduces the kinetic energy of the jet at impingement, resulting in ineffective cutting and inferior part quality. The reduction in SOD and depth

of cut (DOC) has an impact on the deformation wear zone of material removal. Therefore, it is better to have a low SOD value because it produces a smoother surface due to more kinetic energy, which ultimately improves the efficiency of the cutting process.

- **Abrasive Mass Flow Rate:** In the AWJM process, the abrasive mass flow rate is directly correlated with cutting efficiency. Increased abrasive mass flow rate causes a corresponding rise in cut depth as well. When the mass flow rate of the abrasive particles are raised, the jet may easily cut through a workpiece, improving cut surface smoothness and a greater rate of material removal.
- **Traverse Speed:** It is the rate at which the nozzle head travels on the material of interest for carrying out the machining process. For increasing the rate of material removal, high rate of traverse is preferred as this will also reduce the machining time. This is achieved as a result of lesser particles striking the surface per unit time.

1.2.6 Cause-Effect diagram

The cause and effect diagram of different input parameters on output parameters of AWJM has been shown Fig. 1.4. It outlines the various causes that affect the input parameters and their effects on the output parameters of AWJM.

1.2.7 Applications

AWJM has a wide variety of application. Abrasive water jet (AWJ) is economically as well as technically viable which make it suitable for industrial application. Abrasive water jet machining has been used in various industrial fields such as manufacturing industry, civil and construction industry, coal mining, food processing, electronic and cleaning business sectors. AWJM process is often applied to aerospace, automotive, electronics and food industries, mining, etc. Some of the important applications are enumerated below.

- The technology is used to produce parts like fibre glass body components, inside trimming like head liners, trunk liner, door panels and on the outside bumpers as well in the automotive industry.

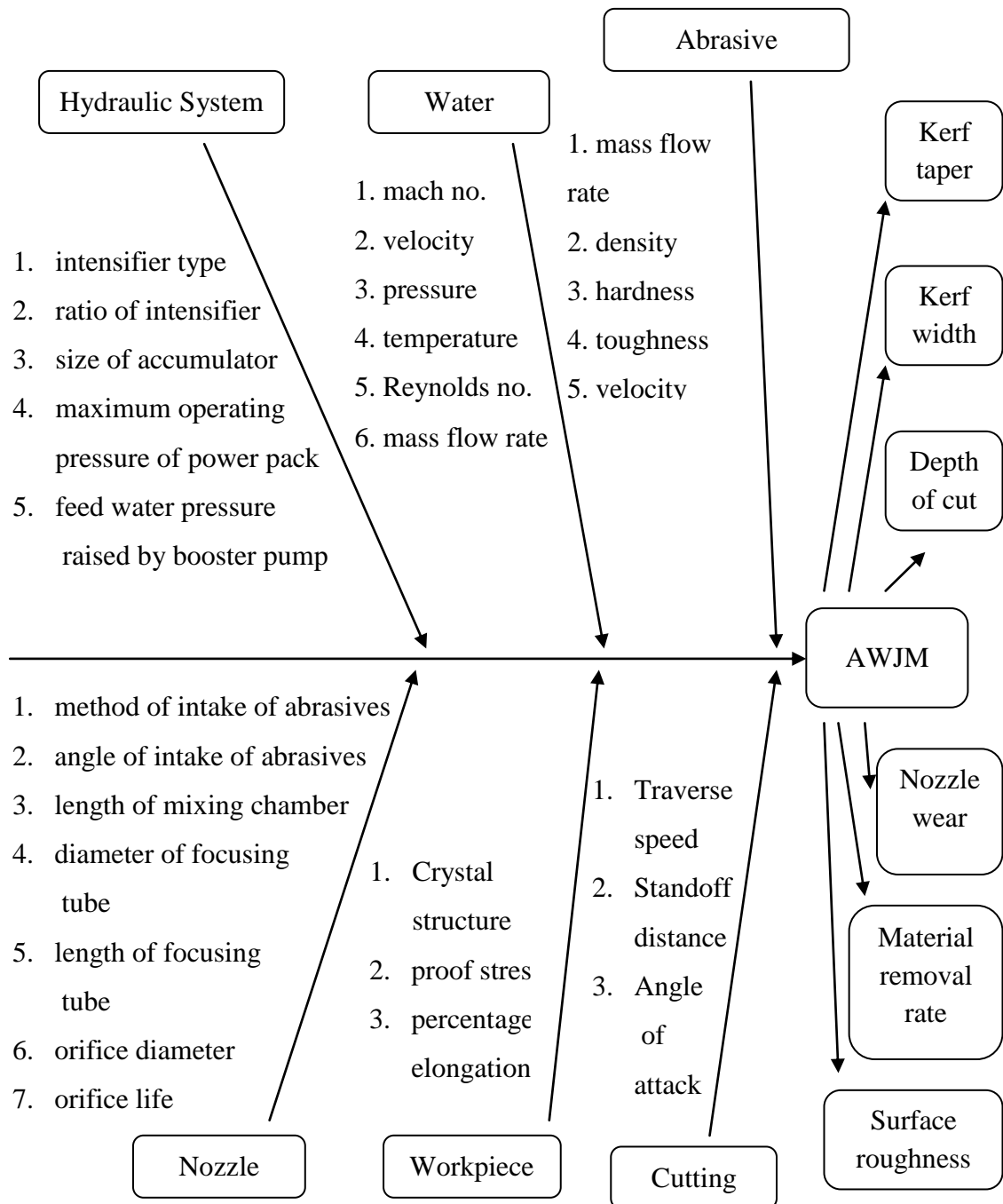


Fig. 1.4: Cause and effect diagram

- In the aerospace industry, the technology is primarily used to manufacture military aircraft body parts made from aluminium, titanium, inner compartment parts plus engine components made from aluminium, titanium, stainless steel and heat-resistant alloys.
- The coal mining sector gets benefitted from AWJM through its capability to cut materials in a safe manner without any hazard.
- AWJM can be used in construction industry as well. This includes a number of applications such as reinforced concrete cutting, etc.
- Within the electronic commerce space, the AWJ cutting technology is widely used for cutting circuit boards from parent larger boards. This is owed to its ability to cut minuscule kerf with very little waste of materials. Circuit board consists of a number of components making it difficult for machining but with AWJM it becomes easier to cut through these crowded intrinsic areas. It is used to manufacture circuit boards and cable stripping as well.
- Rescue operations, pipe cutting, repairs, platform cutting through cutting of casing are some of the examples of use for AWJM within the industry of gas and oil.
- This technology finds its application in food industry too. Preparation of food like trimming meat fats and cutting of bread etc. can be achieved through the ice jet cutting process.

1.2.8 Advantages

The advantages of AWJM technique are multifarious. Some of them are listed below:

- Regardless of the material hardness or any other characteristic, it cuts through any material.
- There is no heat-affected zone, unlike other advanced machining processes such as EBM, LBM, etc.
- Machining costs are comparatively lesser.
- Independent of material hardness and conductivity, it offers great flexibility.
- It is viable to cut thin walled parts as low magnitude machining forces are generated.

- There is minimum material waste.
- There is a lower probability of the environment contamination.
- This process requires no lubrication.
- It is regarded as green or an environmentally friendly process as no toxic fumes are generated during the process.
- It is faster than other methods implying higher rate of production.

1.2.9 Limitations

On the other hand, there are few limitations to this process as well. These are listed below:

- The capital cost of the process is too intensive.
- During the process, it creates a lot of noise.
- Some parts of the equipment have short life spans, i.e., orifice and the nozzle which adds to the cost of overheads and cost of replacement to AWJM operation.
- Inaccurate combination of process parameters can result in undesirable output values of the geometry and surface roughness.

CHAPTER 2

LITERATURE REVIEW & RESEARCH OBJECTIVES

2.1 Literature Review

Mohit Rana et al. [22] established that the transverse speed has a mixed influence on Kerf, but stand-off distance and abrasive flow mass (AMF) are directly related to material removal rate and surface quality. It was also found that MRR improvement resulted in reduced surface finish (SF) and higher Kerf values.

M. Rajesh et al. [23] had conducted several experiments on AWJM on flax fiber stacked laminate and concluded that the pressure and feed rate were found to be the most influenced parameters and had utilized the desirability approach. They deduced that abrasive mass flow rate and water pressure had an indirect effect on the response of surface roughness (Ra).

M.Shunmugasundaram et al. [24] had utilized Taguchi approach for optimizing machine parameters. He concluded that the water pressure has been more dominant parameter over the surface roughness. The abrasive mass flow rate has been more influential than traverse speed for the surface roughness.

Vikas Gulia et al. [25] had inferred from the ANOVA analysis that traverse speed TS has been the most significant factor for achieving minimum Ra and Kerf.

Shalom Akhai et al. [26] had studied the influence of the variable input process parameters. Stand-off distance and abrasive mass flow rate (AFR) were found to be highly significant affecting the MRR but TS had very less effect on surface roughness and negligible effect on kerf in AWJM process for Al-6061. AMF had shown to have a relatively less effect on SF and Kerf as compared to SOD and TS. Also, as the MRR rose, surface roughness and kerf values had fallen.

Chithirai Pon Selvan et al. [27] presented the test of AWJM parameters on mild steel using artificial neural network. The research effect confirms that both water pressure and mass flow rate were directly proportional to depth of cut and surface smoothness. Depth of cut and surface smoothness values decreased when traverse speed and stand-off distance values were increased.

Optimization of Process Parameters in abrasive water jet machining of Nickel Alloy using traditional analysis to minimize kerf taper angle was analyzed by J. Jeykrishnana [28]. Furthermore, effect of input parameters on kerf was also been investigated.

K. Gowthama [29] published the effects of optimizing process parameters of AWJM of Al 7071 by using design of experiments. TS and abrasive moving speed has superior effect on both surface roughness and material removal rate. Also, it was inferred that surface smoothness increases as stand-off distance decreases.

Chandrakant Chaturvedi et al. [30] presented experimental research corroborated with multi-response optimization of process variable in abrasive water jet Machining of Ti-6Al-4V alloy by Taguchi's methodology. It was concluded that the pressure was the most significant parameter followed by SOD, then TS and least is AFR.

Fermin Bañon et al. [31] had done abrasive water jet machining on thermoplastic matrix composites and had concluded that the most influential parameter was hydraulic pressure followed by abrasive mass flow and feed rate. The surface quality at the inlet of the water jet is not affected by the variation in the feed rate, possibly due to the erosion generated.

Waheed Sami Abushanab et al. [32] investigated the influences of input process parameters on surface roughness and topography of the cut surface of Ti6Al4V alloy. It was concluded that the abrasive flow rate contributed 29.32 % and the stand-off distance had 61.77 % contribution in controlling surface roughness as compared to other process parameters.

Bharath Reddy Gunamgari and Manjeet Kharub [33] carried out experiments on high strength aluminum 7068 alloy using garnet 80 mesh abrasive. It was observed that the greatest significant parameter for maximum MRR and lower surface roughness was traverse speed succeeded by abrasive feed rate and SOD.

C. Joel and T. Jeyapoovan [34] used Grey-Taguchi method for determining the predicted optimal parametric combinations and finally the experiment was conducted based on optimized parameters and the cutting accuracy was evaluated. Abrasive feed rate contributed 46.52% in abrasive cutting operation which was followed by nozzle speed with 36.76% contribution and finally came stand-off distance with 15.05% contribution.

K. Karthik et al. [35] concluded from the response graph that material removal rate was influenced by water jet pressure and feed rate while the influencing factors for kerf top width were feed rate and abrasive flow rate.

R. Selvam et al. [36] developed hybrid laminated composite materials with Carbon and S-Glass fibers as primary reinforcement and filler material as SiC nano particles. The effects of process parameters on experimentally obtained quality characteristics values were empirically correlated by generating response surface graphs and then they were optimized within the tested range based on desirability approach of RSM. It was observed that kerf Taper (Kt) decreased with a decrease of both traverse speed and SOD and with a moderate water pressure change.

M. Adam Khan and Kapil Gupta [37] identified the influence of individual process parameters using analysis of variance. Jet travel speed was the predominant factor to be considered for the removal of material. When the jet travelled at maximum speed, the rate of removal was high. Water jet pressure, jet travel speed, and stand-off distance significantly affected kerf wall inclination.

Vootkuri Naveen Reddy & Bellam Venkatesh [38] did optimization of parameters of glass laminate aluminum reinforced epoxy (GLARE). It was concluded that at low abrasive water jet pressure and high SOD, delamination and fiber pull out occurred.

M. Chithirai Pon Selvan et al. [39] did mathematical modeling using Artificial Neural Network on Ti-6Al-4V. It was observed that the model could predict for the new set of data with more than 90% accuracy which could be further used in predicting the output for different set of data for various materials.

Arghya Bagchi et al. [40] studied the impact of distinct parameters on surface roughness and MRR and different surface pattern throughout the thickness of workpiece. It had been noticed that the surface roughness at the bottom portion was reduced at high jet pressure. The high jet pressure, low cutting speed and low SOD improved MRR as well as surface quality.

K. Ravi Kumar et al. [41] carried the investigations on 2, 4, 6, 8 and 10 wt.% Tungsten carbide reinforced composite specimens fabricated by stir casting technique. ANOVA method was employed to check the adequacy of the model developed by RSM. The developed model had good adequacy at 95% level of confidence. MRR was greatly influenced by traverse speed followed by % reinforcement and standoff distance respectively while surface roughness was highly influenced by % tungsten carbide followed by traverse speed and standoff distance respectively were culminated.

Water jet pressure and traversal rate were identified by Srinivas and Babu [42] as elements that helped composites made of aluminium and silicon carbide particulate metal of 70 mm of trapezoidal thickness to attain greater depths of penetration. In order to achieve greater depth of jet penetration by AWJ, they have also highlighted statistical modeling for AWJ cutting of the target material with varying SiC percentage required careful selection of traverse rate and abrasive mass flow rate instead of water jet pressure.

Surface roughness of brass 360 by AWJ machining had been studied by Naresh Babu & Muthukrishnan [43]. According to their findings, water jet pressure had the greatest impact on surface roughness. The kinetic energy of the abrasive particles increased as the water jet pressure rose. As a result, material removal took place. The striations that had formed on the machined surface were lessened by this effect. This resulted in

a smooth finish. With 25% increase in water jet pressure, there was a 33% gain in surface quality.

Iqbal et al.'s [44] examined the AWJ cutting of aluminium 2219 and 4340 tool steel. The work material had a thickness of 20mm and 40mm. They found that reduction in the traverse rate resulted in a smoother surface in the cutting wear zone. By quickening up traversing, kerf width can be decreased. The outcome also showed that the most important variables for hardened material were traverse speed and material thickness.

Kea et.al [52] developed a flexible magnetic abrasive jet machining for examining the machining properties of the self-made magnetic abrasive in abrasive water jet machining. The result drawn from the Taguchi approach was that the flexible magnetic abrasive particles provided better MRR and surface roughness than conventional abrasives.

Wang and fan [53] published a theoretical investigation and supplemented it with mathematical models for the velocity of abrasive particles in an abrasive air jet machining. Air velocity was determined using the Bernoulli's equation for compressible flow. The particle velocity at the nozzle exit was calculated by taking into account the particle mean diameter, nozzle length, air density and air flow. The experimental results were compared with the theoretical calculation to obtain less than 4% error.

Gradeena et.al [54] utilised aluminum oxide as an abrasive for cryogenic abrasive jet machining apparatus for solid particle erosion of polydimethylsiloxane (PDMS). The operating temperature range was kept between -178°C to 17°C. He noticed that ideal machining of PDMS occurred at temperature approximately at -178°C while keeping the impingement angle in between 30° to 60°.

Ally et al. [55] found that while using the 50 μm Al_2O_3 abrasive powder to machine the aluminium 6061-T6, 316L stainless steel and Ti-6Al-4V alloy, the most effective erosion happened at impact angles between 20° and 30°. Using the surface evolution model which was initially developed for ductile polymer, illustrating metal machining

revealed that metal had the lowest AWJM etch rate when compared to glass and polymer.

Tyagi [56] conducted a theoretical analysis with the aid of a mathematical model and computational technique for abrasive water jet machining. By manipulating the input parameters, such as the electric field, magnetic field, and shear scale length, erosion from metallic surfaces could be controlled.

Wang [57] analysed the depth of penetration of alumina ceramics in AWJ with the help of the nozzle oscillation technique. It was found that penetration depth were significant when machined by the single pass cutting with nozzle oscillation. For machining thicker materials, the use of multi pass cutting was also suggested to obtain deeper depth of penetration.

Deepak et al. [58] studied variations of the traverse rate and stand-off distance for the AWJ cutting of D2 steel. They chose kerf width and surface roughness as output parameters. After analysing these two parameters, it was inferred that with an increase in stand-off distance, the top kerf width increased by 18% while bottom kerf width decreased by 25% resulting in kerf taper. Whereas, for the same traverse speed, there was a reduction in kerf taper and surface roughness values. However, kerf taper variability was considerably low.

2.2 Research objective

A number of researches have been done on crystalline brittle materials and ductile materials as well. Keeping in mind aforementioned research works, the cutting behaviour is not clearly comprehended on amorphous materials. Thus, borosilicate glass, an amorphous material has been chosen for the experiment. The aims of the current work are as follows:

- To analyse the experiment during machining of the borosilicate glass.
- To identify the effects of process parameters such as water pressure, stand-off distance, abrasive mass flow rate and traverse speed on material removal rate and radius of curvature of the cut surface.

- To establish the mathematical model and implement process optimization.
- To carry out single and multi objective optimization for material removal rate and radius of curvature.
- Comparative analysis of process responses.

CHAPTER 3

EXPERIMENTAL SETUP

3.1 AWJM System

The equipment used for machining the samples was Flow Mach 3 having 1313B model based on window controlled personal computer software. Abrasive water jet cutting machine was equipped with a hyper jet pump with a maximum pressure of 6500 bar (94,000 psi). The machine had a provision for gravity feed type of abrasive hopper, an abrasive feeder system, with pneumatically controlled valve and a work piece table with dimension of 1219.2×1219.2 mm. The nozzle was regularly inspected throughout the trials and changed with a new one if it was noticeably worn out. Almadine garnet was used as the abrasive for all trials, with a mesh size of #80 (300-150 μ m). The size was preferred because of its profound industrial application.

3.1.1 AWJ machine specifications

Details of the AWJM machine has been shown in the Table 3.1.

3.1.2 Equipments

A typical abrasive water jet system consists of the following major sub systems:

- An intensifier pump to provide high pressure water
- Abrasive feed system
- An abrasive water jet cutting head and a water supply system
- A position control system
- A catcher unit

3.1.2.1 Intensifier Pump

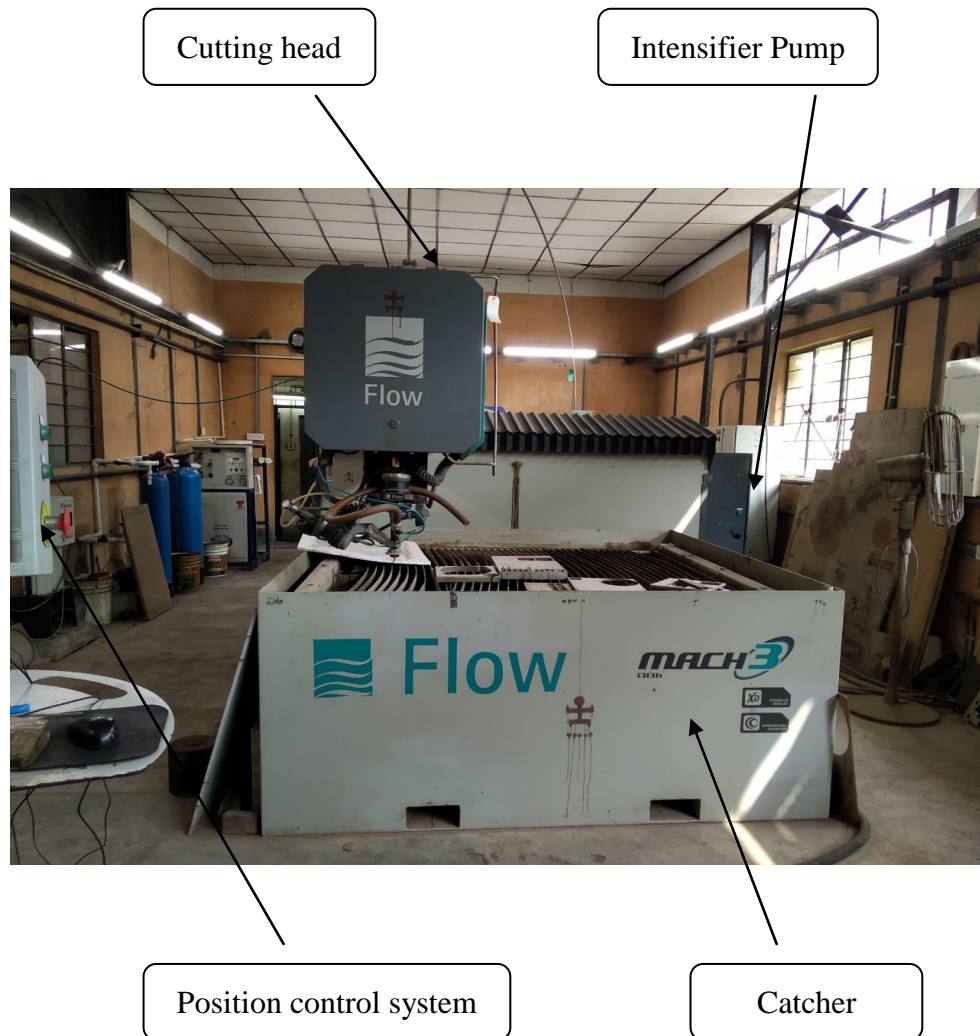
By using intensifier, it can generate high velocity water jet by pressurizing water to a very high magnitude. Water flow requirements till 3 gpm are very common and for getting such a high pressure 75 HP motor may be needed.

Table 3.1: Details of the machine

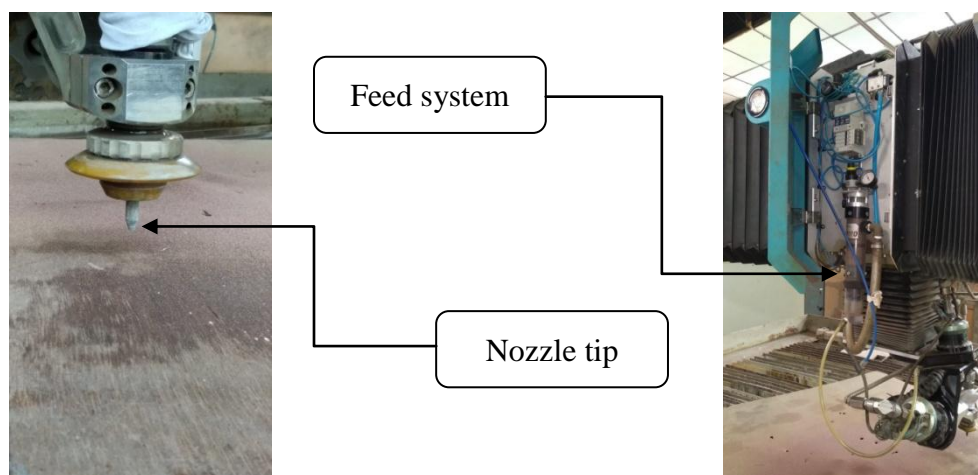
Machine	Flow Mach 3 1313B
Linear Straightness Accuracy	0.0381 mm per 1m
Cut Speed	7.6m/min
Traverse Speed	12.7m/min
Repeatability	0.050 mm
Size	1.3m X 1.3 m
Maximum Pressure	6500 bar (94000 psi)
Orifice Diameter	0.254 mm
Focusing Tube Diameter	0.762 mm
Abrasive Flow Rate	0.36296 kg/min
Numeric Control	Flow Technology
Number Of Motion	5 axis motion
X-Y Cutting Travel Speed	25 m/min
Z Travel	178 mm
B Rotation	-15 degrees to 105 degrees
C Rotation	360 degrees (stationary pierce)
Pump	50HP
Power Supply Voltage	3 X 145/50Hz ($\pm 10\%$)
Axis Movement	AC servo motors with linear guide ways

3.1.2.2 Abrasive Feed System

It is responsible to feed a controlled flow of abrasive particles to the jet nozzle. The current abrasive feed system is providing dry abrasives to the nozzle. In a mixing tube, water flow is responsible to produce enough suction for the flow of the abrasives. By changing the diameter of the controlled orifice, we can change the flow



(a)



(b)



(c)

Fig. 3.1: Complete setup of abrasive water jet machine

rate of abrasives. But by doing so, such system have limitations as they can supply abrasives to a small distance only. To get rid of this limitation, researchers are working on a system in which it will be possible to use abrasive particles directly to get the desired result and mixing of abrasive particles with water will no longer be needed. And by doing so, we can feed slurry to much longer distance though it will require more power than what we require now.

3.1.2.3 Water jet cutting head

It is responsible for performing two tasks namely, mix abrasives and jet water, and produce a high velocity water abrasive jet. It must provide coherent, and focussed abrasive stream while coming out of the nozzle which can be made of sapphire, boron carbide or tungsten carbide. Abrasives fed from the side, mix with water jet in single jet side feed nozzle. This nozzle is easy to make and economical in cost as well but the efficiency in mixing that we are getting here is not optimal. Thus results in wearing out, at the exit part of nozzle. However, in the case of multiple jets, central feed nozzle is comprised of a centrally located abrasive feed system surrounded by multiple jets. It provides better result in mixing abrasives and also provides increased nozzle life. Though, it is highly costly and difficult to make because of the angle of convergence used between the nozzles.

3.1.2.4 Position control system

Position control system is mainly driven by a control algorithm. The control algorithm determines the feed rate change for a particular geometry in a specific material to produce a precise component. In order to give an incredibly high feed rate, the algorithm really determines the desired variability in the tool path and the feed rate.

3.1.2.5 Catcher Unit

The next part of the system is catcher which is a long narrow tube and kept under the point of cut to collect the used jet. It comes in use when material of interest moves and nozzle remains at rest. But when nozzle moves and material of interest remains at

rest then a water carrying tank is placed underneath the targeted material. The used jet gets collected in the tank.

3.2 Flow chart of experiment

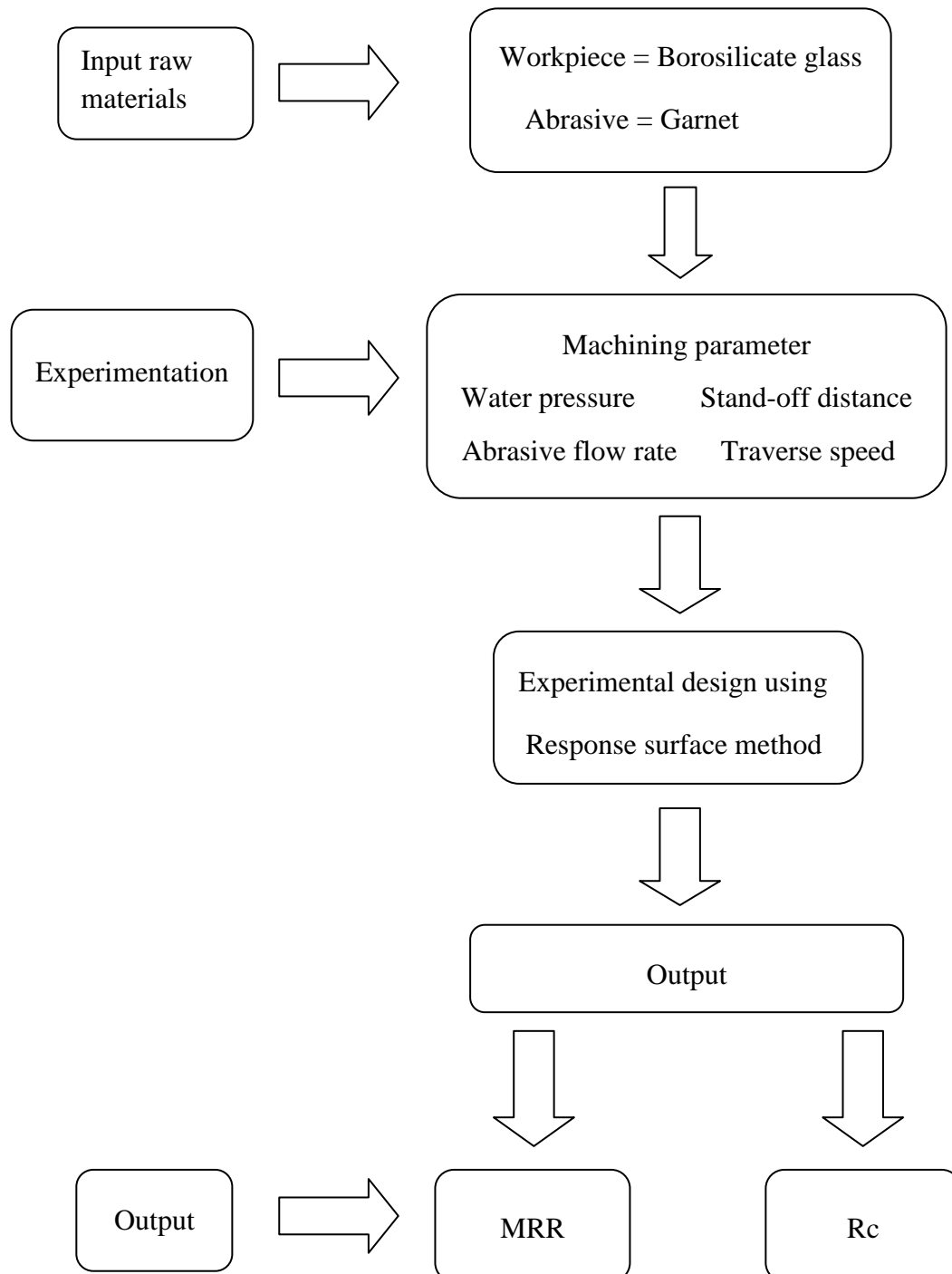


Fig. 3.2: Flow chart of experiment

CHAPTER 4

DESIGN OF EXPERIMENT AND OPTIMIZATION TECHNIQUE

The process of planning the experiments by taking the input process parameters at different levels into account is known as Design of Experiments (DOE). This information can be used to create statistical models which further can be used to guess the process performance beforehand. An experiment whose design comprised of two or more factors each at different possible levels and whose experimental units take into account all possible combinations of these levels across such factors is known as a full factorial experiment, in statistics. Some of the combinations can be neglected in a fractional factorial design, provided the number of combinations in a full factorial design is very high.

For example, per say, there are, 12 factors at two levels, then $2^{12}=4096$ combinations would be generated. . It becomes almost impossible to perform such a large number of experiments as high cost and limited resources comes in the play.

In such cases, fractional factorial designs may be used; but fractional factorial designs are less attractive if a researcher wishes to consider more than two levels. Attempts are made to employ the full factorial design of experiments and analysis of variance approach for studying the influence of process parameters on output responses parameters. Minitab is software, used for both statistics and dynamic response experiment. The goal of robust experimentation is for finding an optimal combination of control factor settings, Minitab is used.

Fractional factorial designs may be employed in these cases but these fractional factorial designs are not much opted, if researcher is going for more than two levels. The full factorial design of experiments and analysis of variance approach is used when one need to study the impact of process parameters on output response parameters. The aim of this rigorous experiment is to find out the outstanding

combinations of the control factor settings and thus Minitab, software used for both statistics and dynamic response experiment is used to reach to the aim. It is easy to use in comparison to others. It comprises of many methods such as Taguchi method, response surface method, factorial, mixture etc.

Basically, there are three types of factor which is responsible for the variation in process response i.e. controllable factor (can be modified during experimentation), signal factors (influence the average values of the response but not its variability). Noise factors (influence on the response but which cannot be controlled). In DOE, we study the effects of multiple factors by performing tests at different levels of the factors. The subjects of discussions in DOE are what the number of experiments we are going to perform, at what levels we are going to perform and how to combine them.

4.1 History of Design of Experiment (DOE)

In order to know the history of DOE, we need to go back in the period of 1920-1930, where Ronald A. Fisher found the DOE, who was an agricultural researcher at Roth Amsted Experimental Station which was stationed 25 miles north of London. Genichi Taguchi, a group of Japanese scientists well known for their quality improvement techniques. These techniques were initially employed by many firms and Toyota is one among them. Ronald A. Fisher described the roots concept behind DOE.

To provide solutions to the problems in experimentation caused by the two types of nuisance factors and to improve the efficiency of experiments, are the fundamental principles in design of experiments. Those are mentioned below:-

- Randomization
- Replication
- Blocking
- Orthogonality

To prevent having influence on the result of experiments from foreign bias is known as randomization. To improve the sample size we follow the method of replication

and hence it results in improving the precision of experiment as well. It improves the signal- to-noise ratio, when uncontrollable nuisance variables start making noises. Starting with the initial setup, it is an exact repeated form of identical experimental conditions known as replication. In case one is finding difficulties in changing a few variables then one can use Split Plot design. To eliminate the effect of known nuisance factors is known as blocking and thus responsible for increasing the experiment precision. The factors are independent of one another in an orthogonal design experiment.

4.2 Uses of DOE

The design of experiment finds its application in the following ways.

- explores interaction among factors
- filter of many factors
- establishment and maintenance of quality control
- process optimization
- making process and/or products robust

Every process has many input variables and has measured output variables accordingly and is regularly examined. Either such processes can be a manufacturing process or a complicated computer simulation method with inputs like pressure, temperature, raw materials etc. The early stage involved in such process known as screening experiment is responsible for identifying which input variables are driving the majority of the variability in the output. A screening experiment, also known as sensitivity analysis or characterisation testing, generally contains only two levels of each factor. In addition to this there is one more term involved in the process which is known as “out of statistical control”-used when the variability or the mean of the process becomes greater than its parameters. However this is a big turn off for the process and the cause of this behaviour must be determined and corrected-which can be done by employing the similar experimental design to screening method. While optimising the process, the shape of the response should be examined. Basically,

significant parameters are first recognised and each parameter has specific levels in a surface design. This details the nature of the surface including peaks, curvature, etc.

4.3 RSM Approach to DOE

One of the modelling and optimisation techniques that is currently popularly used to describe the performance of the machining process and identify the optimal responses of interest is response surface methodology (RSM). When modelling and analysing a response of interest being influenced by numerous variables and the goal is to optimise the response, RSM is a collection of mathematical and statistical techniques that might be helpful. Response surface approach includes the following:

- Creating an experimental plan to investigate the range of the process or independent factors
- Empirical statistical modelling to establish a suitable close to relationship between the output and the process variables
- The process of optimisation involves identifying the values of the process variables that result in optimum response values.

Modelling was started with a second order model because this includes both the interaction and the quadratic terms of independent variables. By this means, any non-linearity or curvature in the response would be considered. General second-order polynomial response surface mathematical model, which is considered to analyze the parametric influences on the response criteria as follows

$$y_u = \beta_0 + \sum_{i=1}^k (\beta_i x_{iu}) + \sum_{i=1}^k (\beta_{ii} x_{iu}^2) + \sum_{i < j} (\beta_{ij} x_{iu} x_{ju}) + e_u$$

where, y_u is the corresponding response, x_{iu} is the coded values of the i th machining parameters for u th experiment, k is the number of machining parameters, β_i , β_{ii} , β_{ij} are the second-order regression coefficients, The residual e_u is a measure of experimental error of the u th observation.

RSM, which is a group of approaches for both regression analysis and experimental design, includes CCD as one of its subtypes. The most popular response surface design is the central composite design (CCD). The response model was created using the multiple linear regression technique. Thirty one trials of a CCD were chosen. In the process modelling, this second order design is capable of handling linear, quadratic, and interaction terms. To have a rotatable design, the interval of levels for each factor is chosen in the design. A design is said to be rotatable if the variation in the response anticipated by the model remains constant at a specific distance from the design's centre, if all parameters are set to their middle level.

Response surface design

Design of the central composite is enumerated below.

- Made from a 2^k factorial design points with multiple additional centre points.
- The distance of the axial runs from the design centre and the number of centre points are two design characteristics that must be stated.
- A face-centred central composite design (CCD) with the parameter = 1.0 can change the standard central composite design's 5 levels for each factor. For each factor, there are just three tiers in the face-centred design.
- The 2^k factorial points were developed for estimating a quadratic model, and they have been used to In order to incorporate the quadratic terms into the first-order model, which has shown a lack of fit, the axial runs are introduced.
- Relatively sensitive to data gaps.
- Near the centre of the design space, where the optimum is thought to be, replicated centre point has excellent prediction capacity.

The value of α depends on the number of experimental runs in the factorial portion of the central composite design:

$$\alpha = [\text{number of factorial runs}]^{1/4} = [2^k]^{1/4}$$

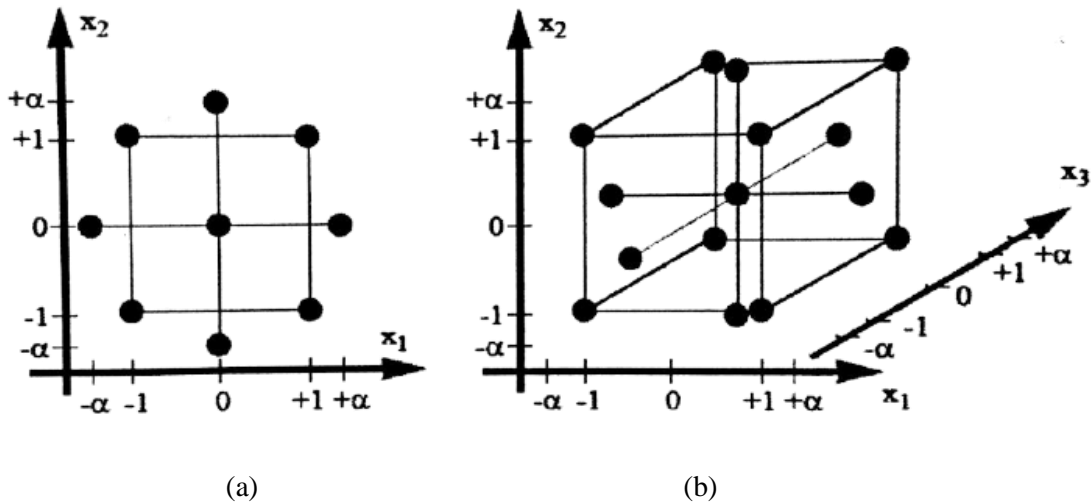


Fig. 4.1: Central composite design points at design space (a) for $k = 2$ and (b) for $k = 3$

4.4 Analysis Of Variance (ANOVA)

With the help of ANOVA, the sum of squares, variance, and percentage contribution of the linear and quadratic effects of the individual parameters and their interaction are determined. These methods were developed by Phadke (1989) and Ross (1989). The error variance can be calculated by combining the sums of squares corresponding to the parameters with the lowest mean square value. It is defined as the ratio of the sum of squares attributable to error to the degree of freedom for error. The variance ratio (F-ratio), often known as the Fisher test or F-test, is the ratio between the mean square owing to a parameter and the error mean square value. To determine if the two variances are equivalent or not, the F-ratio is used. F-ratio can be used to determine the extent of the parameter influence in relation to the error variance. For the purpose of evaluating the process parameter, the F-ratio value is compared with the values from the statistical tables. An F-ratio that is higher than the value in the statistical table indicates that the parameter has an impact on the average population, whereas F-ratios that are lower than the value in the table indicate that the parameter has no impact on the average (Ross 1989; Phadke 1989). This ratio aids in determining the response parameter's degree of confidence. All of the quality traits examined in AWJ machining have undergone ANOVA analysis. These findings were used to identify the significant parameters for building a statistical model.

4.5 Optimization Techniques

Optimization techniques have been deployed to find the optimal values which give the desired output response. These responses either have maximum or minimum values. These techniques help to find the optimal process parameter settings that would lead to the maximum criteria for the output values in this paper. There are a number of approaches to find the optimality condition. Out of all, desirability function approach is most preferred. This is because of its simplicity while others approach mainly focus on optimization of the mean of multi responses.

4.5.1 Desirability function approach (DFA)

The desirability function approach, also known as the utility function approach, is a concept used in decision theory and economics to quantify and compare the desirability or utility of different outcomes or options. It involves assigning numerical values or scores to outcomes based on their perceived desirability or utility to an individual or group. Responses are translated into a corresponding desirability rating, which is how it works. The target's response and range affect the value of attractiveness. When the response achieves its objective, the desired unity value is assigned. The value of desirability is evaluated as zero outside of a specified range.

The geometric mean of each response is the objective composite desirability, or D . The single value of D determines whether or not the combined replies are generally desirable. On a scale of 0 to 1, with 1 being the most attractive, is the composite desirability. Since overall desire is the geometric mean of individual responses, if any one reaction becomes irrational, overall desirability also becomes irrational.

CHAPTER 5

EXPERIMENTAL PLAN AND PROCEDURES

5.1 Experimental Plan

The present experimental study has been performed as per the following:

- The work specimens required to perform the experiments are thirty one in number of the same borosilicate glass material measuring 20 mm × 13 mm × 33 mm.
- For performing abrasive water jet machining, the setup to perform the same is required.
- A mechanical clamping device is used to keep the sample in position which is to be machined.
- To conduct abrasive water jet machining by setting different levels of process parameters such as water pressure, stand-off distance, abrasive mass flow rate and traverse speed. The purpose of conducting the machining is to identify the exact combinations of input process parameters for optimal output.
- Measurement of samples weight, before and after using weighing machine.
- Observation and measurement of the machined surface using scanning electron microscope.

5.2 Work material

5.2.1 Specimen

In this research work, thirty one samples of the same borosilicate glass are considered as the work material for performing the experiments. Particulars of specimen and abrasive particles are given below:

Table 5.1: Mechanical properties of borosilicate glass.

Material	Borosilicate glass
Specimen Size	20 mm × 13 mm × 33 mm
Density	2.28 g/cc
Tensile Strength	81.6 MPa
Young's Modulus	64 GPa
Thermal Conductivity	1.15 W/m.K
Melting Point	1252°C

5.2.2 Abrasive Particles

The abrasive particles employed in the machining process are almandine garnets of mesh size # 80 (300-150 μm).

Table 5.2: Physical and chemical properties of the garnet.

Property	Value
Chemical Formula	$\text{Fe}_3\text{Al}_2(\text{SiO}_4)_3$
Specific Gravity	4.1
Average Bulk Density	2.4 g/cm ³
Hardness	8.0 (mohs scale)
Melting Point	1315 °C

5.3. Experimental Details

5.3.1. Selection of process parameters

Four independently controllable process parameters, namely: water pressure, stand-off distance, abrasive mass flow rate and traverse speed are considered as input parameters to carry out the experiments.

5.3.2. Finding the limits of process parameters

Trial runs were carried out by changing one of the process parameters at a time while keeping the others constant. The upper and lower limits are coded as +2, +1, 0, and -1, -2 respectively. The selected process parameters, their limits, notations and units are given in Table 5.3.

Table 5.3: Parameters with notations, units and levels.

Parameters	Notations	Units	Levels				
			-2	-1	0	1	2
Water pressure	WP	bar	1000	1125	1250	1375	1500
Abrasive mass flow rate	AFR	g/min	18	27	36	45	54
Stand-off distance	SOD	mm	30	37.5	45	52.5	60
Traverse speed	TS	mm/min	200	250	300	350	400

5.3.3. Experimental Design

The experiment is designed using the Central Composite Design (CCD) with full replication at the four factor five level. There will be thirty one experiments. In this design, the four process variables that are under your control are water pressure, abrasive mass flow rate, stand-off distance, and traverse speed. Throughout this experimental work, the garnet size has been kept constant as it is widely used for industrial application. Moreover, changing abrasive type/size in feeder is not feasible. Analysis of variance (ANOVA) was used to see the influence of individual parameters on material removal rate and radius of curvature. The sequential F-test and lack-of-fit test were used to determine whether the established models are acceptable. Utilising the statistical design programme Design-Expert® (Minitab v17), the experimental matrix was created based on the CCD of RSM. The coded and uncoded design matrixes have been shown in Table 5.4 and Table 5.5 respectively.

Table 5.4: Coded design matrix.

Exp. No.	Water Pressure (bar)	Abrasive mass flow rate (g/min)	Traverse speed (mm/min)	Stand-off distance (mm)
1	-1	-1	-1	-1
2	1	-1	-1	-1
3	-1	1	-1	-1
4	1	1	-1	-1
5	-1	-1	1	-1
6	1	-1	1	-1
7	-1	1	1	-1
8	1	1	1	-1
9	-1	-1	-1	1
10	1	-1	-1	1
11	-1	1	-1	1
12	1	1	-1	1
13	-1	-1	1	1
14	1	-1	1	1
15	-1	1	1	1
16	1	1	1	1
17	-2	0	0	0
18	2	0	0	0
19	0	-2	0	0
20	0	2	0	0
21	0	0	-2	0
22	0	0	2	0
23	0	0	0	-2
24	0	0	0	2
25	0	0	0	0
26	0	0	0	0
27	0	0	0	0
28	0	0	0	0
29	0	0	0	0
30	0	0	0	0
31	0	0	0	0

Table 5.5: Uncoded design matrix

Exp. No.	WP (bar)	AFR (g/min)	TS (mm/min)	SOD (mm)
1	1125	27	250	37.5
2	1375	27	250	37.5
3	1125	45	250	37.5
4	1375	45	250	37.5
5	1125	27	350	37.5
6	1375	27	350	37.5
7	1125	45	350	37.5
8	1375	45	350	37.5
9	1125	27	250	52.5
10	1375	27	250	52.5
11	1125	45	250	52.5
12	1375	45	250	52.5
13	1125	27	350	52.5
14	1375	27	350	52.5
15	1125	45	350	52.5
16	1375	45	350	52.5
17	1000	36	300	45
18	1500	36	300	45
19	1250	18	300	45
20	1250	54	300	45
21	1250	36	200	45
22	1250	36	400	45
23	1250	36	300	30
24	1250	36	300	60
25	1250	36	300	45
26	1250	36	300	45
27	1250	36	300	45
28	1250	36	300	45
29	1250	36	300	45
30	1250	36	300	45
31	1250	36	300	45

5.4 Experimental Procedure

The procedure for carrying out the AWJ machining is explained below.

- The workpiece was fixed on the AWJ work area using the fixtures available on the work area.
- The workpiece were cut to a length of 20 mm.
- The specimens were cut to a width of 13 mm.
- Each specimen was labelled using numbers (1, 2, 3, 4,...) to distinguish the different specimens.
- Weights of the specimens before machining were taken.
- The AWJ machining was performed after a dry run test on the specimen.
- The part program and the process parameters were loaded to the CNC.
- After the AWJ cut has been performed, the specimens were washed and dried.
- Weights of the specimens after machining were taken.
- One side of the cut channel was separated into a size of 1 cm X 1 cm and was analysed.



Fig.5.1: Machined borosilicate glass

5.5 Testing Equipments

5.5.1 Scanning electron microscope

The scanning electron microscope (SEM) creates images using electrons. The SEM's broad depth of field enables it to focus on a sizable portion of the material. High-resolution images are produced by SEM, which enables high magnification. Since the sample surface can now be accurately represented in three dimensions, the SEM is able to provide this image. The accelerated electrons in SEM, act as light in vacuum. They can have wavelengths that are shorter than those of light and move in straight lines. The SEM can magnify objects up to 400000 times at a resolution of 1 nm. An electron beam is produced by an electron gun (cathode) at the top of the column in a scanning electron microscope. The beam is drawn towards the anode, condensed by collimator lenses, and focussed on the sample by objective lenses. Electrons are taken from the filament and propelled towards the anode by using an electric potential difference between the anode and the filament. In a SEM, the primary electrons that are created when the specimen is struck by the primary beam are recognised and converted into an electrical signal. The primary electrons are then converted into light to create an image on the fluorescent screen. When electrons collide, they can

- Be reflected.
- Emit X-rays from the specimen whose energy and wavelengths are associated with its elemental content.
- Emit secondary electrons, which are electrons that are emitted by the specimen itself

In order to analyze closely the cut surface generated by AWJ, SEM analysis was performed. The Analysis was carried out at different magnifications of the cut surfaces, viewing in depth the typical streaks created by the AWJ technology. Radius of curvature of the striation marks on the cut sample of each sample was measured from the photographs taken through microscope. Radius of curvature was measured by three-point circle method. Photographs at different positions of a typical sample

cut under optimum control parameter settings are taken under scanning electron microscope (Make: JOEL, Model: JSM-6360).

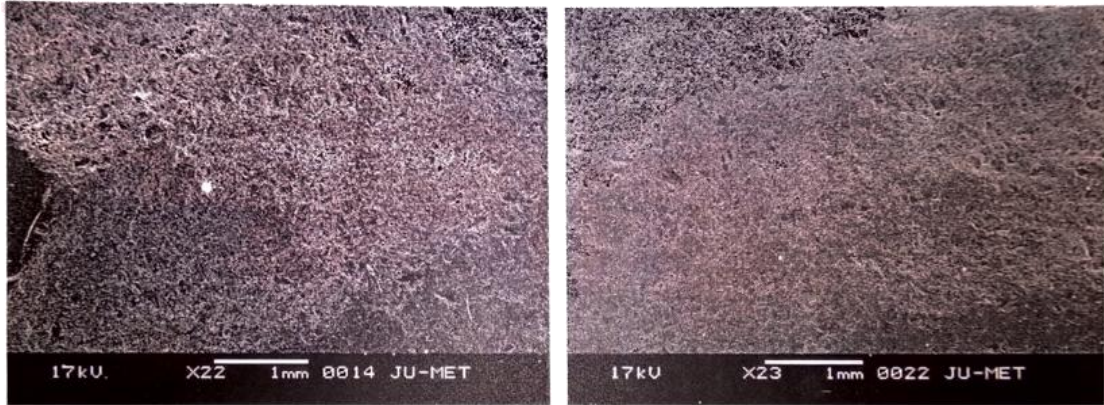


Fig. 5.2: Striation marks on cut surface

5.5.2 Weighing machine

Weighing machine is a device used to measure weight or mass. The MRR is defined as the volume of material removed from work piece per unit time.

The MRR is calculated as the ratio of the difference of weight of the workpiece before and after machining to the machining time to obtain the MRR in terms of g/min.

$$MRR = \frac{WB - WA}{t}$$

Where,

WA = Weight of work piece after machining, gm

WB = Weight of work piece before machining, gm

t = Machining time, min

The loss in weight was measured by measuring balance (Make: SARTORIUS AG GERMANY, CPA 10035, Model: 26109103) with accuracy of 0.001g.

CHAPTER 6

EXPERIMENTAL INVESTIGATION AND OPTIMIZATION

This chapter deals with the experimental findings and outcomes of the performed experiment and also aims to find the impact of process factors on MRR and Rc. In this ongoing chapter, observed data have been studied for mathematical modelling, optimization and response surface plots. While working with constrained resources, the design of experiments has been employed to increase the MRR and Rc. Empirical models have been developed so that one can demonstrate the relationship between process parameters and response. These models often used in knowing the optimum response conditions for the given optimization criteria, where the output characteristics are at their desired values. The impact of individual parameter on MRR and Rc have been observed and the best suitable conditions are known.

6.1 Experimental Results

The process of selection of appropriate process parameters and developing the design matrix for the experiment using Minitab v17 software was done. Abrasive water jet machining was performed for right combinations of input process parameters as designed by the RSM technique's central composite design. The experiment was performed and the measurements were noted. These have been shown in Table 6.1.

6.2 Development of Mathematical Models Using RSM

For a given set of input parameters, RSM is used to create mathematical models that forecast the results. The built-in models are evaluated for their suitability using the analysis of variance (ANOVA) method. The establishment of relationships between the input and the output parameters are necessary to comprehend the behaviour of the process. ANOVA is used to develop the relationship among input and output characteristics. The relationship between two or more interesting variables can be

examined using regression analysis, a potent statistical method. Regression analysis is used to precisely estimate the most crucial components, as well as secondary factors that can be disregarded and their interactions.

Table 6.1: Design matrix and measured experimental results.

Exp. No.	WP (bar)	AFR (g/min)	TS (mm/min)	SOD (mm)	MRR (g/min)	Rc (mm)
1	1125	27	250	37.5	8.01	6.98
2	1375	27	250	37.5	9.44	11.96
3	1125	45	250	37.5	10.4	7.34
4	1375	45	250	37.5	11.88	13.27
5	1125	27	350	37.5	8.85	6.52
6	1375	27	350	37.5	10.4	9.37
7	1125	45	350	37.5	11.54	6.81
8	1375	45	350	37.5	12.77	10.02
9	1125	27	250	52.5	6.56	6.62
10	1375	27	250	52.5	8.04	8.17
11	1125	45	250	52.5	9	6.99
12	1375	45	250	52.5	10.58	9.27
13	1125	27	350	52.5	7.45	6.27
14	1375	27	350	52.5	8.93	7.01
15	1125	45	350	52.5	9.68	6.18
16	1375	45	350	52.5	11.37	7.85
17	1000	36	300	45	7.56	6.23
18	1500	36	300	45	11.22	12.76
19	1250	18	300	45	7.98	8.16
20	1250	54	300	45	12.01	8.88
21	1250	36	200	45	9.68	8.96
22	1250	36	400	45	10.58	6.86
23	1250	36	300	30	11.06	9.03
24	1250	36	300	60	7.27	6.19
25	1250	36	300	45	10.89	8.22
26	1250	36	300	45	10.24	8.12
27	1250	36	300	45	10.68	8.59
28	1250	36	300	45	10.5	7.89
29	1250	36	300	45	10.66	8.55
30	1250	36	300	45	10.44	8.06
31	1250	36	300	45	10.19	8.19

6.2.1 Analysis of material removal rate (MRR)

Table 6.2 shows the ANOVA results for material removal rate with a confidence level of 95%. Using ANOVA, it has been observed from the Table that abrasive flow rate appears to have the greatest impact on MRR, followed by standoff distance and water pressure which have similar impact. Traverse speed has the least impact. As a result, this equation is appropriate for quadratic equations with curvature on the response surface. The developed mathematical model of MRR in terms of uncoded factors, is given below:

$$\begin{aligned} \text{MRR} = & -44.8 + 0.0495 \text{ WP} + 0.253 \text{ AFR} + 0.0351 \text{ TS} + 0.422 \text{ SOD} - 0.000018 \\ & \text{WP}^2 - 0.001579 \text{ AFR}^2 - 0.000038 \text{ TS}^2 - 0.005961 \text{ SOD}^2 + 0.000002 \\ & \text{WP} \cdot \text{AFR} - 0.000000 \text{ WP} \cdot \text{TS} + 0.000036 \text{ WP} \cdot \text{SOD} - 0.000011 \text{ AFR} \cdot \text{TS} - 0.00023 \\ & \text{AFR} \cdot \text{SOD} - 0.000097 \text{ TS} \cdot \text{SOD} \end{aligned}$$

The model adequacy measures, namely R^2 , adjusted R^2 and predicted R^2 are found to be equal to 0.9814, 0.9652, and 0.9159 respectively, which are very close to unity. The very close agreement of R^2 values indicates that the developed model is adequate. The lack-of-fit F-value is not significant relative to the pure error, and this is desirable.

6.2.2 Analysis of radius of curvature (Rc)

Table 6.3 shows the ANOVA results for radius of curvature with a confidence level of 95%. Using ANOVA, it is observed from the Table that water pressure appears to have the greatest impact on Rc, followed by standoff distance. As a result, this equation is appropriate for quadratic equations with curvature on the response surface. The developed mathematical model of Rc in terms of uncoded factors, is given below:

$$\begin{aligned} \text{Rc} = & -34.1 + 0.0125 \text{ WP} - 0.132 \text{ AFR} + 0.0782 \text{ TS} + 0.951 \text{ SOD} + 0.000018 \\ & \text{WP}^2 + 0.000439 \text{ AFR}^2 - 0.000047 \text{ TS}^2 - 0.00341 \text{ SOD}^2 + 0.000165 \\ & \text{WP} \cdot \text{AFR} - 0.000063 \text{ WP} \cdot \text{TS} - 0.000715 \text{ WP} \cdot \text{SOD} - 0.000201 \text{ AFR} \cdot \text{TS} - 0.00036 \\ & \text{AFR} \cdot \text{SOD} + 0.000515 \text{ TS} \cdot \text{SOD} \end{aligned}$$

Table 6.2: Analysis of variance for MRR.

Source	DF	Adj SS	Adj MS	F-Value	P-Value
Model	14	70.99	5.07	60.43	0
Linear	4	65.84	16.46	196.18	0
WP	1	15.39	15.39	183.44	0
AFR	1	31.7	31.7	377.84	0
TS	1	3.27	3.27	39.01	0
SOD	1	15.47	15.47	184.41	0
Square	4	5.1	1.27	15.19	0
WP*WP	1	2.23	2.23	26.62	0
AFR*AFR	1	0.47	0.47	5.57	0.03
TS*TS	1	0.25	0.25	3.02	0.1
SOD*SOD	1	3.22	3.22	38.32	0
2-Way Interaction	6	0.04	0.01	0.09	1
WP*AFR	1	0	0	0	0.98
WP*TS	1	0	0	0	0.98
WP*SOD	1	0.02	0.02	0.21	0.65
AFR*TS	1	0	0	0	0.95
AFR*SOD	1	0	0	0.04	0.84
TS*SOD	1	0.02	0.02	0.25	0.62
Error	16	1.34	0.08		
Lack-of-Fit	10	0.97	0.1	1.54	0.31
Pure Error	6	0.38	0.06		
Total	30	72.33			
Model Summary		S	R-sq	R-sq (adj)	R-sq (pred)
		0.29	98.14%	96.52%	91.59%

Table 6.3: Analysis of variance for Rc.

Source	DF	Adj SS	Adj MS	F-Value	P-Value
Model	14	96.63	6.9	57.29	0
Linear	4	81.53	20.38	169.18	0
WP	1	54.81	54.81	454.96	0
AFR	1	1.64	1.64	13.6	0
TS	1	9.09	9.09	75.45	0
SOD	1	15.99	15.99	132.72	0
Square	4	4.15	1.04	8.62	0
WP*WP	1	2.23	2.23	18.52	0
AFR*AFR	1	0.04	0.04	0.3	0.59
TS*TS	1	0.39	0.39	3.24	0.09
SOD*SOD	1	1.05	1.05	8.74	0.01
2-Way Interaction	6	10.94	1.82	15.14	0
WP*AFR	1	0.55	0.55	4.58	0.05
WP*TS	1	2.46	2.46	20.39	0
WP*SOD	1	7.2	7.2	59.73	0
AFR*TS	1	0.13	0.13	1.09	0.31
AFR*SOD	1	0.01	0.01	0.08	0.78
TS*SOD	1	0.6	0.6	4.95	0.04
Error	16	1.93	0.12		
Lack-of-Fit	10	1.54	0.15	2.36	0.15
Pure Error	6	0.39	0.07		
Total	30	98.55			
Model Summary		S	R-sq	R-sq (adj)	R-sq (pred)
		0.35	98.04%	96.33%	90.48%

The model adequacy measures, namely R^2 , adjusted R^2 and predicted R^2 are found to be equal to 0.9804, 0.9633, and 0.9048 respectively, which are very close to unity. The very close agreement of R^2 values indicates that the developed model is adequate. The lack-of-fit F-value is not significant relative to the pure error, and this is desirable.

6.3 Process Parameters Effects on Outputs

6.3.1 Effects of process parameters on material removal rate

The combined effect of abrasive mass flow rate and traverse speed is shown in Fig. 6.1. Water pressure and stand-off distance were taken as constant at 1250 bar and 45 mm respectively. It was observed that material removal rate increases with increase in traverse rate at all the levels of AFR. This was due the reason that abrasive water jet covers more length over the surface of the workpiece and hence more material got removed from the workpiece thereby increasing MRR.

It was also observed that material removal rate increases with increase in abrasive mass flow rate at all the levels of traverse speed. As the AFR was increased more abrasive particles came into picture. These particles were responsible for cutting of the workpiece. Since more and more abrasive particles were involved, therefore there has been more cutting action in unit time i.e. increased number of cutting edges resulting in higher MRR.

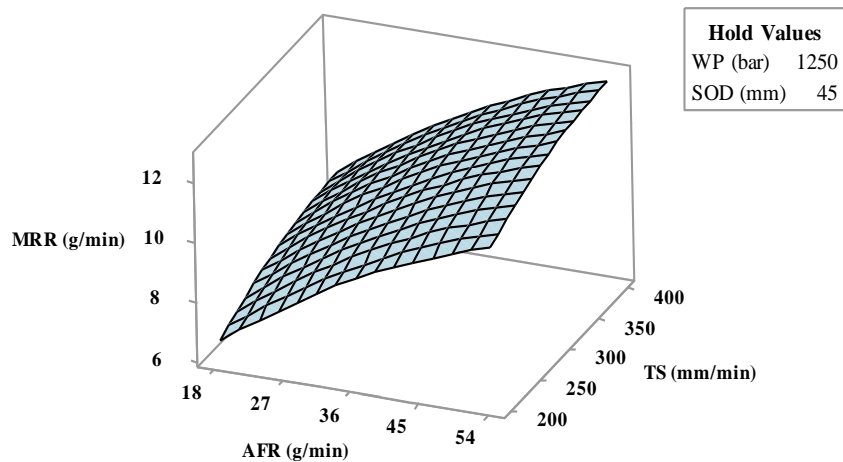


Fig. 6.1: Response surface of MRR with AFR and TS

The combined effect of water pressure and stand-off distance is shown in Fig. 6.2. Abrasive mass flow rate and traverse speed were taken as constant at 36 g/min and 300 mm/min respectively. It was observed that material removal rate increases with increase in water pressure and then started decreasing at higher pressure values at all

the levels of abrasive mass flow rate. This was due to the reason that with increase in the pressure jet velocity increased, which directly influenced the kinetic energy of abrasive particles impinging on the work material which led to a higher removal of material. But at higher pressure values, large pressure resulted in more suction of abrasive particles which resulted in collision of the abrasive particles among themselves. This resulted in loss of kinetic energy thereby decreasing the MRR value.

It was also observed that material removal rate increases with decrease in stand-off distance at all levels of WP. This was due to the reason that with increase in stand-off distance, jet expansion and external drag from the surrounding environment both resulted in reducing the kinetic energy of the abrasives. This resulted in lesser impact on the work material thereby decreasing MRR. At higher SOD, the liquid phase of the jet broke up into droplets resulting in free abrasive particles. These abrasive particles rebounded upon impact that further led to lower MRR. After a particular value of SOD, MRR decreased slightly due to insufficient distance to impact the material properly and hence inefficient cutting was observed. And then increases to give higher MRR values.

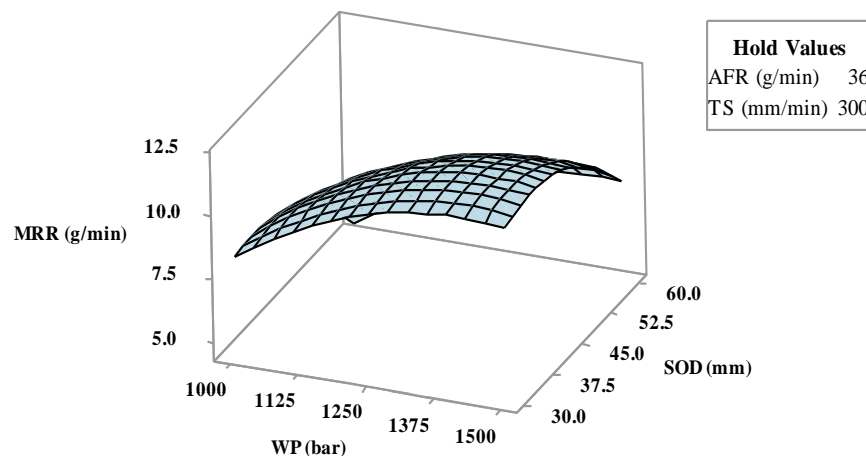


Fig. 6.2: Response surface of MRR with WP and SOD

The combined effect of stand-off distance and traverse speed on MRR is shown in Fig. 6.3. Water pressure and abrasive mass flow rate were taken as constant at 1250 bar and 36 g/min respectively. It was observed that an increase in TS resulted in increase of MRR at all the levels of SOD. This was due to the reason that abrasive

water jet covers more length over the surface of the workpiece resulting in higher value of MRR. It can also be inferred from the graph that SOD first increases slightly and then decreases at all the levels of TS. Initially, when nozzle is very close to material, it results in inefficient cutting. When SOD was increased, MRR first increased then decreased owing to decrease in jet energy.

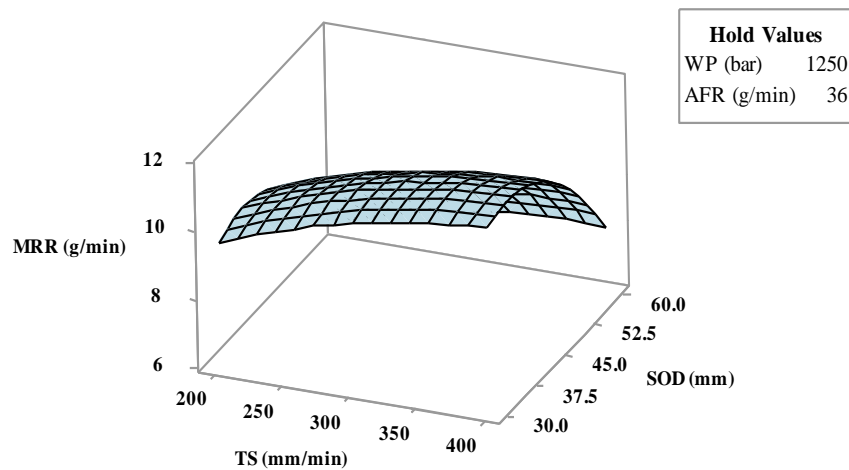


Fig. 6.3: Response surface of MRR with TS and SOD

The effect of stand-off distance and abrasive mass flow rate on MRR is shown in Fig. 6.4. Water pressure and traverse speed were taken as constant at 1250 bar and 300 mm/min respectively. At all levels of SOD, it was found that MRR rises as AFR rises. Increased AFR led to higher abrasive particle mass flow rates, which allowed for more effective cutting. The graph also implied that MRR initially climbs modestly and subsequently declines with SOD. Initially, ineffective cutting occurred when the nozzle was placed very close to the material. Therefore, with slight increased value of SOD, the MRR was observed at a higher value.

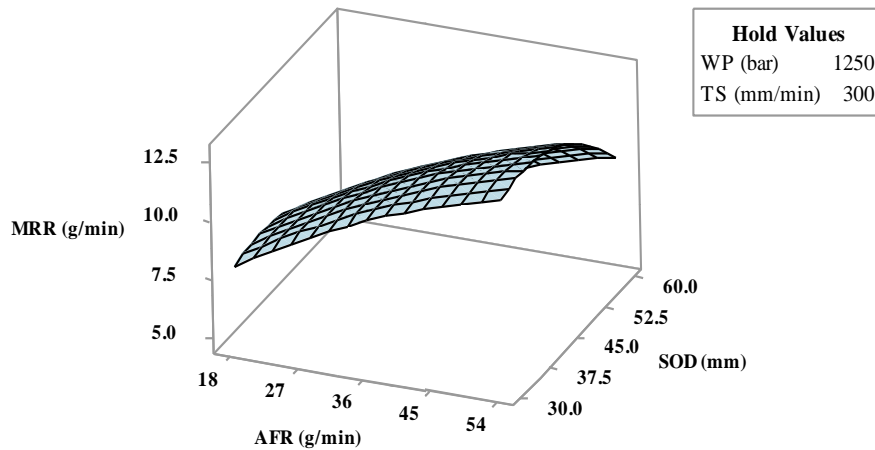


Fig. 6.4: Response surface of MRR with AFR and SOD

The effect of traverse speed and water pressure on MRR is shown in Fig. 6.5. Abrasive mass flow rate and stand-off distance were taken as constant at 36 g/min and 45 mm respectively. It was determined that for all levels of TS, MRR rises with an increase in water pressure before gradually falling off. This occurred as a result of rising jet velocity due to the increased pressure, which also altered the kinetic energy of abrasive particles impacting the work material and boosted material removal. However, as pressure increases, there has been a greater tendency for abrasive particles to suction together, which resulted in abrasive particle collision. Due to the loss of kinetic energy, the MRR value decreased.

From the graph, it can also be seen that MRR increases with increase in TS as higher speed enables more material removal from the workpiece. Higher value of water pressure combined with higher TS value resulted in increased MRR.

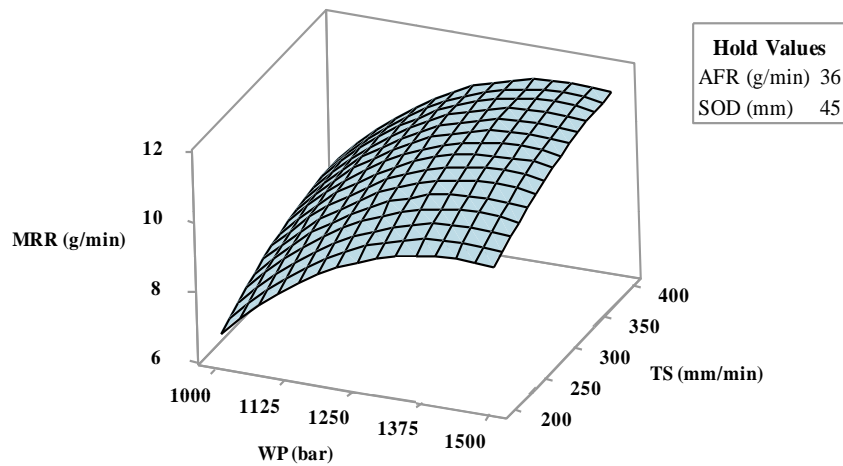


Fig. 6.5: Response surface of MRR with TS and WP

The combined effect of water pressure and abrasive mass flow rate and is shown in Fig. 6.6. Traverse speed and stand-off distance were taken as constant at 300 mm/min and 45 mm respectively. It was observed that MRR increases and then decreases slightly with increasing WP at all levels of AFR. Also, MRR increases with AFR at all the levels of WP. At higher pressure, AFR influences the MRR more and thus higher water pressure combined with increased AFR resulted in higher MRR.

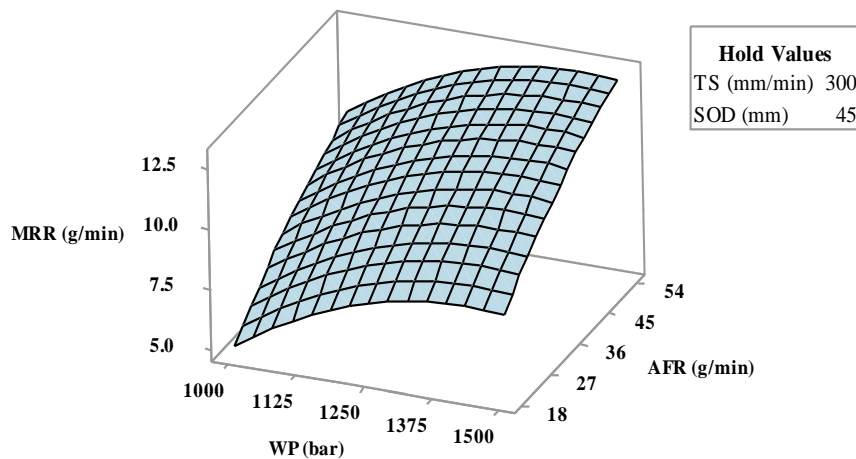


Fig. 6.6: Response surface of MRR with WP and AFR

6.3.2 Effects of process parameters on radius of curvature

The combined effect of abrasive mass flow rate and water pressure on radius of curvature is shown in Fig. 6.7. Traverse speed and stand-off distance were taken as constant at 300 mm/min and 45 mm respectively. It was observed that radius of curvature increases with increase in water pressure at all the levels of AFR. This was due to the reason that the radius of bend marked on the workpiece reflects the resistance of the material against the erosion of high energy abrasive jet. As, the energy of the jet increased with increasing water pressure, cutting ability also increased, so jet exited with a large bend i.e. large radius of curvature. It was also observed that with increase in abrasive mass flow rate, radius of curvature also increases at all levels of water pressure. This was due to the reason that when AFR increases, more abrasive particles were involved in cutting thereby increasing cutting ability. This resulted in large bend.

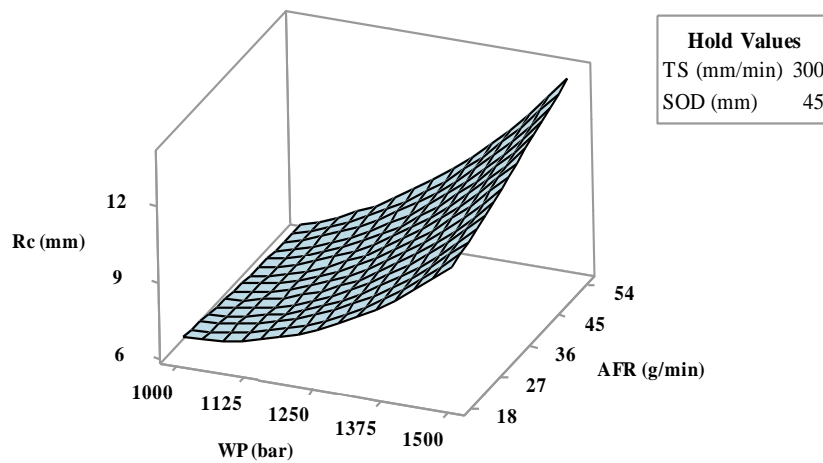


Fig. 6.7: Response surface of R_c with WP and AFR

The combined effect of traverse speed and stand-off distance is shown in Fig. 6.8. Abrasive mass flow rate and water pressure were taken as constant at 1250 bar and 36 g/min respectively. It was observed that radius of curvature decreases with increase in traverse speed at all the levels of SOD. When the jet traversed with higher speed, rate of energy supplied decreased which caused sharp jet deflection. This sharp deflection resulted in small radius of curvature. It was also observed that with increase in stand-off distance, radius of curvature also decreased at all levels of water pressure. This

was due to the reason that with increase in standoff distance, the energy of jet decreased which caused smaller radius of curvature. However, when SOD was increased from a extreme lower value where cutting was inefficient, R_c increased as jet possessed higher energy and jet diversion was less as jet was extremely focused resulting in larger bend.

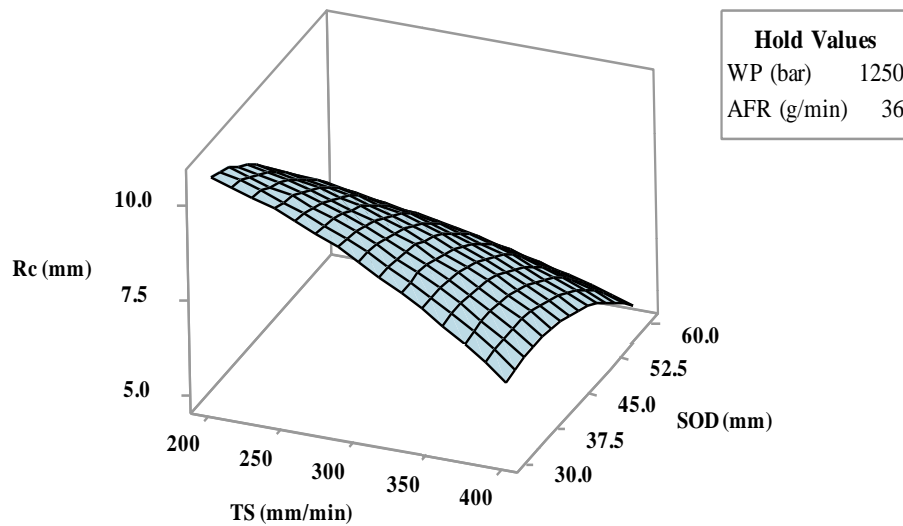


Fig. 6.8: Response surface of R_c with TS and SOD

The effect of traverse speed and abrasive mass flow rate on R_c is shown in Fig. 6.9. Water pressure and stand-off distance were taken as constant at 1250 bar and 45 mm respectively. It can be easily seen that R_c increased with increase in abrasive mass flow rate and it first increased slightly and then decreased with traverse speed. Higher value of abrasive mass flow rate and lower traverse speed value together resulted in maximum radius of curvature as evident from the graph as well. This was due to increased cutting action at higher abrasive flow rate and increased rate of supplied jet energy at lower traverse speed.

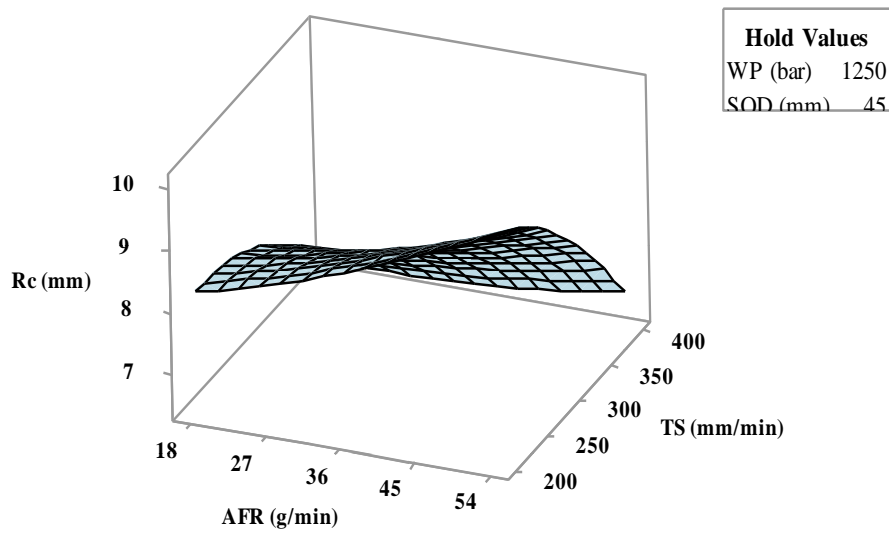


Fig. 6.9: Response surface of Rc with AFR and TS

The effect of water pressure and stand-off distance on Rc is shown in Fig. 6.10. AFR and TS were taken as constant at 36 g/min and 300 mm /min respectively. It is clear from the graph that Rc increased as WP was increased and it decreased with SOD. It can be conferred that higher WP and lower SOD has been desired for large bend. However at extremely lower SOD, cutting action was not significant and hence lower Rc was observed.

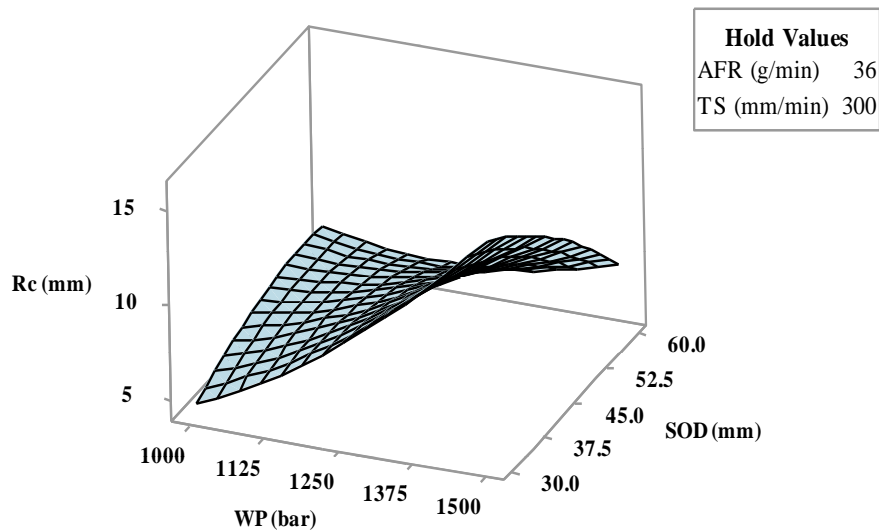


Fig. 6.10: Response surface of Rc with WP and SOD

The effect of abrasive mass flow rate and stand-off distance on radius of curvature is shown in Fig. 6.11. Water pressure and traverse speed were taken as constant at 1250 bar and 300 mm/min respectively. It was found that Rc rises with rising abrasive mass flow rate and falling stand-off distance. As can be seen from the graph as well, a considerable bend was produced by increased abrasive mass flow rate and lower stand-off distance. However, due to the increased rate of energy delivered, a considerable bend was seen at extremely low stand-off distance.

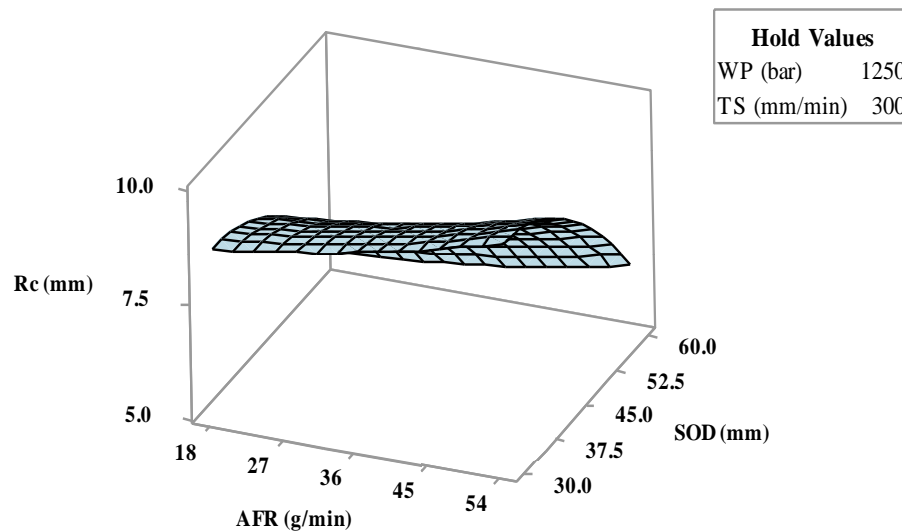


Fig. 6.11: Response surface of Rc with SOD and AFR

The effect of water pressure and traverse speed is shown in Fig. 6.12. Abrasive mass flow rate and stand-off distance were taken as constant at 36 g/min and 45 mm respectively. Higher water pressure and lower traverse speed were found to cause greater bends, which is also clear from the graph. Because of the extremely high energy associated with the jet, huge values of Rc were attained at increased water pressure, even at traversal rates that were lower.

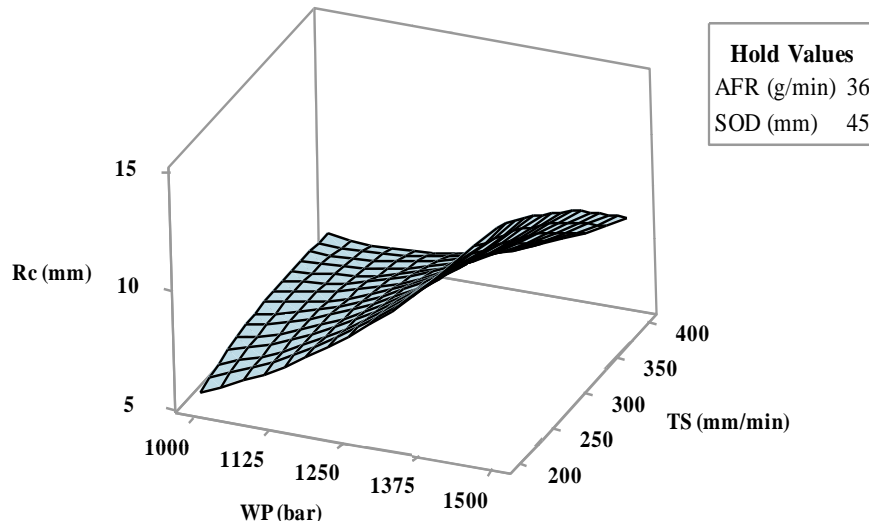


Fig. 6.12: Response surface of Rc with WP and AFR

6.4 Optimization of Process Parameters

In this part, effort is made to optimize the material removal rate and radius of curvature for abrasive water jet machining of borosilicate glass. Single-objective optimization and multi-objective optimization were performed and they have been compared together with desirability function approach (DFA).

6.4.1 Single-objective optimization

Finding the best values for a group of input variables or parameters in order to maximise or minimise a single goal or performance indicator is known as single-objective optimisation (SOO). A statistical method known as Response Surface Methodology (RSM) is used to model and examine the relationship between input factors and response variables. Finding the ideal set of input variables that maximises or minimises the response variable predicted by the response surface model is what SOO entails in the context of RSM. Minitab v17 software has been used to obtain optimum responses in abrasive water jet machining on borosilicate glass.

In this process, initially, single-objective optimization is done, where material removal rate and radius of curvature are optimized independently. The aim is to maximize the material removal rate and radius of curvature as well.

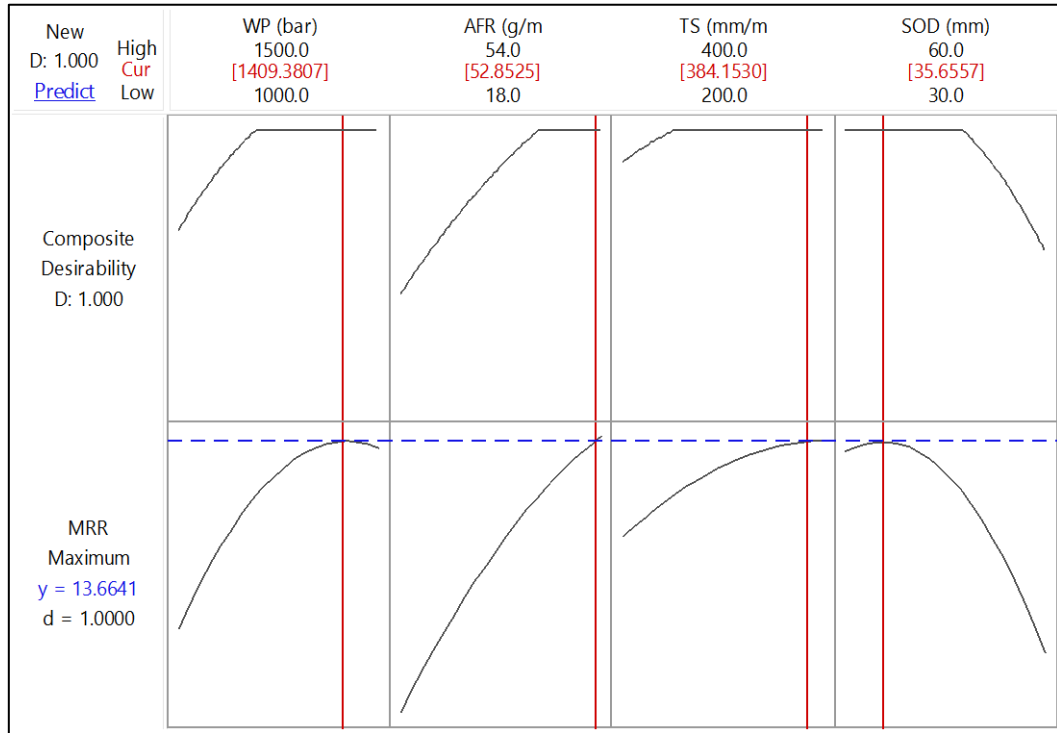


Fig. 6.13: Optimization result for material removal rate

The optimization results for maximum material removal rate based on the developed mathematical model (RSM) are shown in Fig. 6.13. The value count for linear desirability function (D) remains to be 1 i.e., all parameters are within their working limit. Maximum material removal rate has been achieved as 13.6641 g/min when water pressure is 1409.3807 bar, abrasive mass flow rate is 52.8525 g/min, traverse speed is 384.1530 mm/min and stand-off distance is 35.6557 mm.

The optimization results for maximum radius of curvature based on the developed mathematical model (RSM) are shown in Figure 6.14. The value count for linear desirability function (D) remains to be 1 i.e., all parameters are within their working limit. Maximum radius of curvature has been achieved as 18.0560 mm when water pressure is 1471.3115 bar, abrasive mass flow rate is 51.2787 g/min, traverse speed is 219.4900 mm/min and standoff distance is 33.6885 mm.

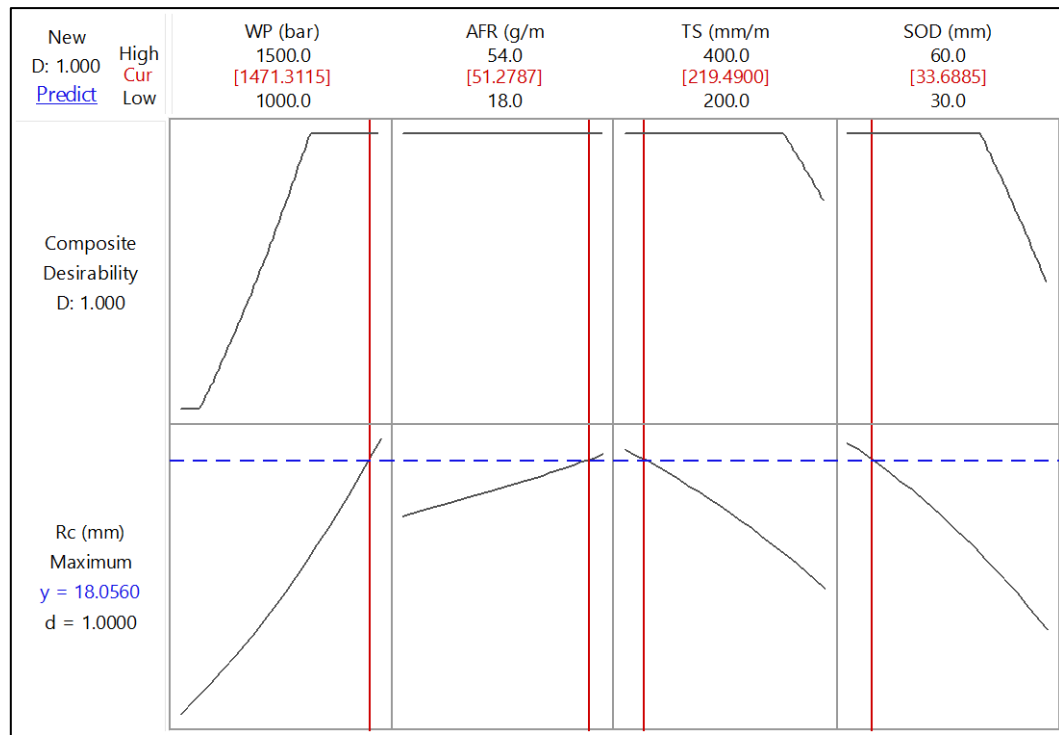


Fig. 6.14: Optimization result for radius of curvature

6.4.2 Multi-objective optimization

The term "multi-objective optimisation" (MOO) refers to the process of determining the best values for a group of input parameters or variables in order to simultaneously optimise a number of competing objectives or performance measures. A statistical method known as Response Surface Methodology (RSM) can be expanded to deal with multi-objective optimisation issues. Finding the ideal set of input variables that concurrently optimises a number of the response variables predicted by the response surface models is known as MOO in the context of RSM. The optimisation findings are validated by comparison with the outcomes of the desirability function approach (DFA).

Fig. 6.15 shows the optimization results for MRR and Rc. Here these two responses have been optimized together in one setting. In multi-objective optimization, the aim is to maximize the material removal rate and radius of curvature simultaneously. Each row of the graph corresponds to a response variable and each column corresponds to

one of the parameters considered during abrasive water jet machining of borosilicate glass. Each cell of the graph shows how one of the response variables changes as a function of one of the parameters, keeping other parameters constant. The vertical line inside the graph represents current parameter settings and a horizontal dotted line represents the current response values. The numbers displayed at the top of a column show the current parameter level settings, high value of that parameter and low value of that parameter setting in the experimental design. At the left side of each row, goal for the response (maximum for MRR and maximum for Rc), predicted response (y) at current parameter settings, and individual desirability scores are given.

The current parametric settings are water pressure is 1445.8106 bar, abrasive mass flow rate is 54 g/min, traverse speed is 351.5152 mm/min and stand-off distance is 32.1585 mm for achieving the predicted maximum value of Rc of 13.3296 mm and maximum value of MRR of 13.5626 g/mm. The composite desirability factor (D) is displayed in the upper left corner of the graph and the value of composite desirability factor is 1.

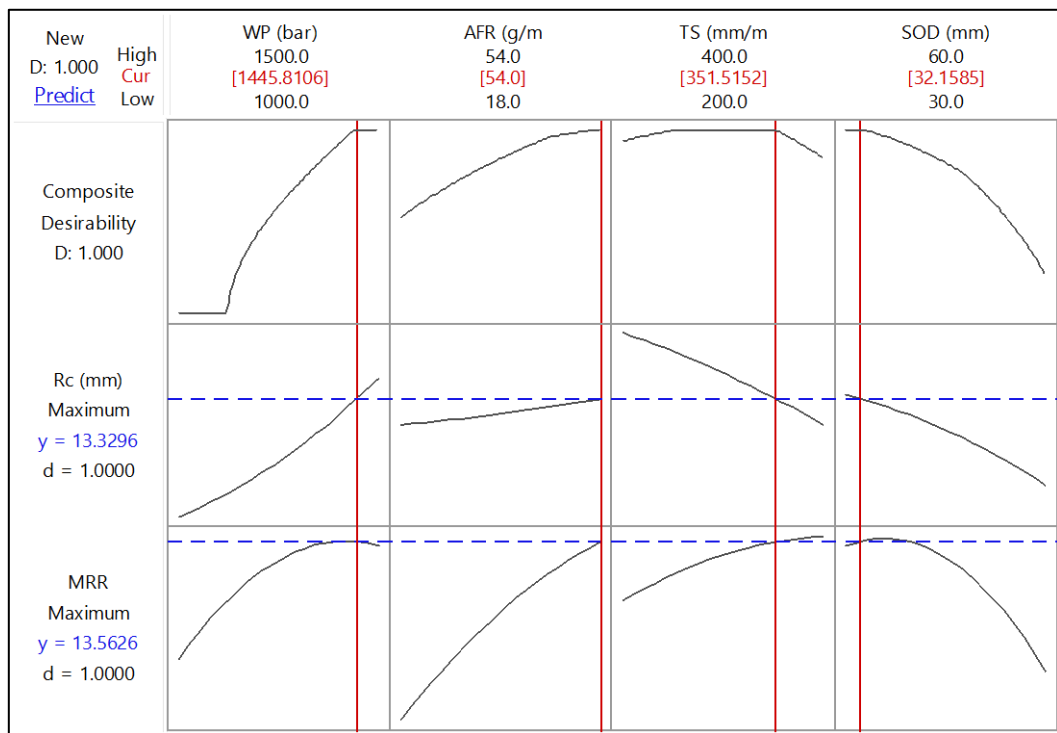


Fig. 6.15: Multi-objective optimization results

6.5 Confirmation Test

To validate the model, three numbers of experiments were conducted for MRR, Rc and MRR & Rc taking into consideration the parameter settings obtained from the single-objective optimization for MRR, Rc and multi-objective optimization results for MRR & Rc respectively.

These experimental results have been compared with the predicted optimum results. It was observed that predicted values are close to the experimental results. The experimental results and the predicted optimum results along with the prediction error have been shown in Table 6.4.

Table 6.4: Final verification experiments.

Machining responses	Predicted value at optimal parametric settings	Experimental value at optimal parametric settings	% of error
MRR (g/min)	13.66	12.63	7.54
Rc (mm)	18.06	17.10	5.32
MRR (g/min), Rc (mm)	13.56, 13.33	12.23, 12.78	9.81, 4.35

CHAPTER 7

CONCLUSION

7.1 Conclusion

Abrasive water jet machining of borosilicate glass has been carried out and effects of different process parameters on response variables have been explained in detail. Single-objective as well as multi-objective optimization analysis of process parameters such as abrasive mass flow rate, water pressure, stand-off distance and traverse speed have also been done. It can be concluded that, the various process parameters i.e. abrasive mass flow rate, water pressure, standoff distance and traverse speed can be optimally controlled for achieving desired responses by using the developed mathematical model based on RSM during abrasive water jet machining of borosilicate glass. The analysis of variance (ANOVA) test has also been done to identify the process parameters that contributed the most to get desired material removal rate and radius of curvature.

In abrasive water jet machining of borosilicate glass, after analyzing the experiment following conclusions have been drawn.

- MRR increases with increasing water jet pressure, abrasive mass flow rate and traverse speed while it decreases with increasing stand-off distance. However, it is also concluded that at extremely lower value of SOD, MRR further decreases slightly due to insufficient distance to impact the material properly and hence leading to inefficient cutting.
- Rc increases with increasing water jet pressure, abrasive mass flow rate while it decreases with increasing stand-off distance and traverse speed. However, when SOD increases from an extreme lower value where cutting was inefficient, jet possess higher energy and jet diversion is also less as the jet is extremely focused resulting in large bend.
- Abrasive mass flow rate has the most significant effect on material removal rate followed by water pressure and stand-off distance.

- For radius of curvature, water pressure is the most significant parameter followed by stand-off distance.
- For single-objective optimization, the MRR value is obtained as 13.6641 g/min while the input parameters value are, water pressure is 1409.3807 bar, abrasive mass flow rate is 52.8525 g/min, traverse speed is 384.1530 mm/min and stand-off distance is 35.6557 mm.
- For single-objective optimization of the Rc, its optimum value is obtained as 18.0560 mm while the input parameters value are, water pressure is 1471.3115 bar, abrasive flow rate is 51.2787 g/min, traverse speed is 219.4900 mm/min and stand-off distance is 33.6885 mm.
- For multi-objective optimization, the optimum values of two responses i.e. MRR and Rc are obtained as 13.5626 g/min and 13.3296 mm respectively when input parameters are, water pressure is 1445.8106 bar, abrasive flow rate is 54 g/min, traverse speed is 351.5152 mm/min and stand-off distance is 32.1585 mm.

7.2 Future Scope of Work

The future work of the present work as understood by author is enumerated as follows:

- Variation mean inclination angle and mean depth of cut are required to be modelled for further better study of the influence of control parameters.
- Water behaves incompressible above the pressure 3800 bar. At high pressure water will not act only as a carrier fluid, it will also erode material. So, combined effect of water and abrasive particles on both crystalline and amorphous material should be studied.
- The characteristics due to radius of curvature need to be studied further to completely understand its impact on the machined work surface.
- Applications of AWJM for boring and turning may be investigated.
- Study of burr formation in AWJM is to be done.
- Application of AWJM in cutting vertically may be investigated.

References

1. A.M. Omer, Sustainable development and environmentally friendly energy systems, *Int. J. Phys. Sci. Eng.*, Volume 1, Issue 1, Pages 1–39, (2017), doi: 10.21744/ijpse.v1i1.2.
2. Ameer M, Hadj Djilani A, Zitoune R, et al., Experimental and numerical investigations of the damages induced while drilling flax/epoxy composite, *Journal of Composite Materials*, Volume 56, Issue 2, Pages 295-312, (2022), doi: 10.1177/00219983211055825.
3. Khashaba UA, Abd-Elwahed MS, Najjar I, Melaibari A, Ahmed KI, Zitoune R, Eltaher MA, heat-affected zone and mechanical analysis of GFRP composites with different thicknesses in drilling processes polymers, Volume 13, Issue 14, Page 2246, (2021), doi: 10.3390/polym13142246.
4. Shunmugasundaram M, Maneiah D, Lingampalle, Mangesha, Nagaraj, Chettya, Patil, Prajwalkumarb, An optimization of process parameters for stir cast aluminium metal matrix composites to improve material removal rate, *International Journal of Mechanical and Production Engineering Research and Development*, Volume 9, Issue 5, Page 951, (2019), doi 10.1016/j.matpr.2020.01.128.
5. Jagadish, Bhowmik, S. & Ray, A. Prediction and optimization of process parameters of green composites in AWJM process using response surface methodology, *Int. J Adv Manuf. Technol.*, Volume 87, Pages 1359–1370, (2016), doi: 10.1007/s00170-015-8281-x.
6. Z. Maros, Energy approach of the taper at abrasive water jet cutting, *Production processes and systems*, Volume 6, Issue 1, Pages 89-96, (2013).
7. Ahmet Hascalik, Ulaş Çaydaş, Hakan Gürün, Effect of traverse speed on abrasive water jet machining of Ti–6Al–4V alloy, *Materials & Design*, Volume 28, Issue 6, Pages 1953-1957, (2007), doi: 10.1016/j.matdes.2006.04.020.
8. Seo, Y. W., Ramulu, M., & Kim, D., Machinability of titanium alloy (Ti’6Al’4V) by abrasive water jets, *Proc. Inst. Mech. Eng., Part B: J. Eng. Manuf.*, Volume 217, Issue 12, Pages 1709-1721, (2003), doi: 10.1243/095440503772680631.

9. Kong, M. C., & Axinte, D. 'Response of titanium aluminide alloy to abrasive water jet cutting: geometrical accuracy and surface integrity issues versus process parameters, *Proc. Inst. Mech. Eng., Part B: J. Eng. Manuf.*, Volume 223, Issue 1, Pages 19-42, (2009), doi: 10.1243/09544054JEM1226.
10. E. Uhlmann, F. Sammler, S. Richarz, F. Heitmüller, M. Bilz, *Machining of Carbon Fiber Reinforced Plastics, Procedia CIRP*, Volume 24, Pages 19-24, (2014), doi: 10.1016/j.procir.2014.07.135.
11. MM, I.W., Azmi, A., Lee, C. et al., Kerf taper and delamination damage minimization of FRP hybrid composites under abrasive water-jet machining, *Int. J Adv Manuf. Technol.*, Volume 94, Pages 1727–1744, (2018), doi: 10.1007/s00170-016-9669-y.
12. Li, H., Wang J., An experimental study of abrasive water jet machining of Ti-6Al-4V, *Int. J Adv Manuf. Technol.*, Volume 81, Pages 361–369, (2015), doi: 10.1007/s00170-015-7245-5.
13. J. Wang, W.C.K. Wong, A study of abrasive water jet cutting of metallic coated sheet steels, *International Journal of Machine Tools and Manufacture*, Volume 39, Issue 6, Pages 855-870, (1999), doi: 10.1016/S0890-6955(98)00078-9.
14. H.C. Meng, K.C. Ludema, Wear models and predictive equations: their form and content, *Wear*, Volumes 181–183, Part 2, Pages 443-457, (1995), doi: 10.1016/0043-1648(95)90158-2.
15. Hashish M., Visualization of the abrasive-water jet cutting process, *Experimental Mechanics*, Volume 28, Pages 159–169, (1988), doi: 10.1007/BF02317567.
16. IM Hutchings, Mechanisms of the erosion of metals by solid particles, *Erosion: prevention and useful applications, J ASTM Int.*, Pages 59–76, (1979), doi: 10.1520/STP35795S.
17. J.G.A. Bitter, A study of erosion phenomena part I, *Wear*, Volume 6, Issue 1, Pages 5-21, (1963), doi: 10.1016/0043-1648(63)90003-6.
18. J.G.A. Bitter, A study of erosion phenomena: Part II, *Wear*, Volume 6, Issue 3, Pages 169-190, (1963), doi: 10.1016/0043-1648(63)90073-5.

19. G.L. Sheldon, I. Finnie, The mechanism of material removal in the erosive cutting of brittle materials, *J Inst Eng*, Volume 88, Issue 4, Pages 393–9, (1966), doi: 10.1115/1.3672667.
20. Che C.L., Huang C.Z., Wang J, Zhu H.T., Study of abrasive water jet polishing technology, *Key Eng Materials*, Volume 487, Pages 327–331, (2011), doi: 10.4028/www.scientific.net/KEM.487.327.
21. Natarajan Yuvaraj & Murugasen Pradeep Kumar, Study and evaluation of abrasive water jet cutting performance on AA5083-H32 aluminum alloy by varying the jet impingement angles with different abrasive mesh sizes, *Machining Science and Technology*, Volume 21, Issue 3, Pages 385-415, (2017), doi: 10.1080/10910344.2017.1283958.
22. Mohit Rana, Shalom Akhai, Multi-objective optimization of Abrasive water jet Machining parameters for Inconel 625 alloy using TGRA, *Materials today proceedings*, Volume 65, Part 8, Pages 3205-3210, (2022), doi: 10.1016/j.matpr.2022.05.374.
23. M. Rajesh , K. Rajkumar , R. Vijayakumar , K. Ramraji, Investigation and optimization of AWJM on flax fiber stacked laminate by desirability approach, *Materials today proceedings*, Volume 62, Part 2, Pages 1146-1151, (2022), doi: 10.1016/j.matpr.2022.04.339.
24. M.Shunmugasundaram, M. Yadi Reddy , A. Praveen Kumar , K. Rajanikanth, Optimization of machining parameters by Taguchi approach for machining of aluminium based metal matrix composite by abrasive water jet machining process , *Materials today proceedings* ,Volume 47, Part 17, Pages 5928-5933, (2021), doi: 10.1016/j.matpr.2021.04.479.
25. Vikas Gulia , Aniket Nargundkar, Experimental investigations of abrasive water jet machining on hybrid composites, *Materials today proceedings*, Volume 65, Part 8, Pages 3191-3196, (2022), doi: 10.1016/j.matpr.2022.05.372.
26. Shalom Akhai, Mohit Rana, Taguchi-based grey relational analysis of abrasive water jet machining of Al-6061, *Materials today proceedings*, Volume 65, Part 8, Pages 3165-3169, (2022), doi: 10.1016/j.matpr.2022.05.361.

27. Chithirai Pon Selvan , Divya Midhunchakkaravarthy, Swaroop Ramaswamy Pillai, Sahith Reddy Madara, Investigation on abrasive water jet machining conditions of mild steel using artificial neural network, Materials today proceedings, Volume 19, Part 2, Pages 233-239, (2019), doi: 10.1016/j.matpr.2019.06.757.
28. J. Jeykrishnana, B. Vijaya Ramnatha, S. Sree Vignesha, P. Sridharana, B. Saravanana, Optimization of Process Parameters in Abrasive Water Jet Machining /Cutting (AWJM) of Nickel Alloy using Traditional Analysis to Minimize Kerf Taper Angle, Materials today proceedings, Volume 16, Part 2, Pages 392-397, (2019), doi: 10.1016/j.matpr.2019.05.106.
29. K. Gowthama , H.M. Somashekar , B. Suresha , Sangamesh Rajole , N. Ravindran, Optimization of abrasive water jet machining process parameters of Al 7071 using design of experiments, Materials today proceedings, Volume 52, Part 3, Pages 2102-2108, (2022), doi: 10.1016/j.matpr.2021.12.380.
30. Chandrakant Chaturvedi, P. Sudhakar Rao, Mohd. Yunus Khan, Optimization of process variable in abrasive water jet Machining (AWJM) of Ti-6Al-4V alloy using Taguchi methodology, Materials today proceedings, Volume 47, Part 17, Pages 6120-6127, (2021), doi: 10.1016/j.matpr.2021.05.040.
31. Fermin Bañon, Alejandro Sambruno, Raul Ruiz-Garcia, Jorge Salguero, Pedro F. Mayuet , Study of the influence of cutting parameters on surface quality in AWJM machining of thermoplastic matrix composites, Procedia Manufacturing, Volume 41, Pages 233-240, (2019), doi: 10.1016/j.promfg.2019.07.051.
32. Waheed Sami Abushanab, Essam B. Moustafa, Mooli Harish, S. Shanmugan, Ammar H. Elsheikh, Experimental investigation on surface characteristics of Ti6Al4V alloy during abrasive water jet machining process, Alexandria Engineering Journal, Volume 61, Issue 10, Pages 7529-7539, (2022), doi: 10.1016/j.aej.2022.01.004.
33. Bharath Reddy Gunamgari, Manjeet Kharub, Experimental investigation on abrasive water jet cutting of high strength aluminum 7068 alloy, Mater. Today Proc., Volume 69, Issue 2, Pages 488-493, (2022), doi: 10.1016/j.matpr.2022.09.180.

34. C. Joel, T. Jeyapoovan, Optimization of machinability parameters in abrasive water jet machining of AA7075 using Grey-Taguchi method, *Mater. Today Proc.*, Volume 37, Issue 2, Pages 737-741, (2021), doi: 10.1016/j.matpr.2020.05.741.
35. K. Karthik, David Smith Sundarsingh, M. Harivignesh, R. Gopi Karthick, M. Praveen, Optimization of machining parameters in abrasive water jet cutting of stainless steel 304, *Mater. Today Proc.*, Volume 46, Issue 2, Pages 1384-1389, (2021), doi: 10.1016/j.matpr.2021.02.489.
36. R. Selvam, N. Arunkumar, L. Karunamoorthy, An investigation on machining characteristics in abrasive water jet machining of hybrid laminated composites with SiC nano particles, *Mater. Today: Proc.*, Volume 39, Issue 4, Pages 1701-1709, (2021), doi: 10.1016/j.matpr.2020.06.193.
37. M. Adam Khan, Kapil Gupta, Machining Ni-Cr-Fe based superalloy using abrasive water jet cutting process and its surface studies, *Mater. Today Proc.*, Volume 19, Issue 5, Pages 2139-2143, (2019), doi: 10.1016/j.matpr.2019.07.227.
38. Vootkuri Naveen Reddy, Bellam Venkatesh, Optimization of parameters in abrasive water jet machining of glass laminate aluminium reinforced epoxy (GLARE), *Mater. Today Proc.*, Volume 19, Issue 2, Pages 890-894, (2019), doi: 10.1016/j.matpr.2019.08.245.
39. M. Chithirai Pon Selvan, Divya Midhunchakkaravarthy, Rohan Senanayake, Swaroop Ramaswamy Pillai, Sahith Reddy Madara, A mathematical modelling of Abrasive Water jet Machining on Ti-6Al-4V using Artificial Neural Network, *Mater. Today Proc.*, Volume 28, Issue 2, Pages 538-544, (2020), doi: 10.1016/j.matpr.2019.12.215.
40. Arghya Bagchi, Madhulika Srivastava, Rupam Tripathi, Somnath Chattopadhyaya, Effect of different parameters on surface roughness and material removal rate in abrasive water jet cutting of Nimonic C263, *Mater. Today Proc.*, Volume 27, Issue3, Pages 2239-2242, (2020), doi: 10.1016/j.matpr.2019.09.104.
41. K. Ravi Kumar, V.S. Sreebalaji, T. Pridhar, Characterization and optimization of Abrasive Water Jet Machining parameters of Aluminium/Tungsten carbide

- composite, *Measurement*, Volume 117, Pages 57-66, (2018), doi: 10.1016/j.measurement.2017.11.059.
42. Srinivas S, Babu NR, Role of garnet and silicon carbide abrasives in abrasive water jet cutting of aluminum-silicon carbide particulate metal matrix composites, *Int. J. Appl. Res Mech.*, Volume 1, Pages 109–22, (2011), doi: 10.47893/IJARME.2011.1022.
 43. Naresh Babu M, Muthukrishnan N, Investigation on surface roughness in abrasive water-jet machining by the response surface method, *Mater Manuf. Processes*, Volume 29, Issue 11–12, Pages 1422–8, (2014), doi: 10.1080/10426914.2014.952020.
 44. Iqbal A, Dar NU, Hussain G, Optimization of abrasive water jet cutting of ductile materials, *J Wuhan Univ. Technol.-Mater Sci. Ed.*, Volume 26, Issue 1, Pages 88–92, (2011).
 45. Yakub Iqbal Mogul, Irfan Nasir, Dr. Peter Myler, Investigation and optimization for depth of cut and surface roughness for control depth milling in Titanium Ti6AL4V with abrasive water jet cutting, *Materials Today Proceedings*, Volume 28, Part 2, Pages 604-610, (2020), doi: 10.1016/j.matpr.2019.12.229.
 46. D.A. Axinte, B. Karpuschewski, M.C. Kong, A.T. Beaucamp, S. Anwar, D. Miller, M. Petzel, High Energy Fluid Jet Machining (HEFJet-Mach): From scientific and technological advances to niche industrial applications, *CIRP Annals*, Volume 63, Issue 2, Pages 751-771, (2014), doi: 10.1016/j.cirp.2014.05.001.
 47. R. Senthil Kumara, S. Gajendranb, R. Kesavanc, Estimation of Optimal Process Parameters for Abrasive Water Jet Machining Of Marble Using Multi Response Techniques, *Materials Today Proceedings*, Volume 5, Issue 5, Part 2, Pages 11208-11218, (2018), doi: 10.1016/j.matpr.2018.01.145.
 48. A.K. Chaitanya, D. Kishore Babu, K.V.N. Girish Kumar, Experimental study on surface roughness by using abrasive jet machine, *Materials Today Proceedings*, Volume 23, Part 3, Pages 453-457, (2020), doi: 10.1016/j.matpr.2019.05.343.
 49. M. Adam Khan, Kapil Gupta, Machining Ni-Cr-Fe based superalloy using abrasive water jet cutting process and its surface studies, *Materials Today*

- Proceedings, Volume 19, Part 5, Pages 2139-2143, (2019), doi: 10.1016/j.matpr.2019.07.227.
50. M. Chithirai Pon Selvan, N. Mohana Sundara Raju, H. K. Sachidananda, Effects of process parameters on surface roughness in abrasive water jet cutting of aluminium, *Front. Mech. Eng.*, Volume 7, Issue 4, Pages 439–444, (2012), doi: 10.1007/s11465-012-0337-0.
 51. M. A. Azmir & A. K. Ahsan & A. Rahmah, Effect of abrasive water jet machining parameter on aramid fiber reinforced plastics composite, *Int. J. Mater Form*, Volume 2, Pages 37–44, (2009), doi: 10.1007/s12289-008-0388-2.
 52. Jiuan-Hung Kea, Feng-Che Tsaia, Jung-Chou Hungb, Biing-Hwa Yanc, Characteristics study of flexible magnetic abrasive in abrasive jet machining, *Procedia CIRP*, Volume 1, Pages 679–680, (2012), doi: 10.1016/j.procir.2012.05.025.
 53. H.Z. Li, J. Wang, J.M. Fan, Analysis and modelling of particle velocities in micro-abrasive air jet, *International Journal of Machine Tools & Manufacture*, Volume 49, Issue 11, Pages 850–858, (2009), doi: 10.1016/j.ijmachtools.2009.05.012.
 54. A.G. Gradeena, J.K. Spelta, M. Papinia, Cryogenic abrasive jet machining of polydimethylsiloxane at different temperatures, *wear*, Volume 274-275, Pages 335-344, (2012), doi: 10.1016/j.matpr.2018.02.293.
 55. S. Ally , J.K. Spelt , M. Papini, Prediction of machined surface evolution in the abrasive jet micro-machining of metal, *Wear*, Volume 292-293, Pages 89-99, (2012), doi: 10.1016/j.wear.2012.05.029.
 56. R.K. Tyagi, Abrasive jet machining by means of velocity shear instability in plasma, *Journal of manufacturing process*, Voume 14, Pages 323-327, (2012), doi: 10.1016/j.jmapro.2012.05.004.
 57. Wang J., A focused review on enhancing the abrasive water jet cutting performance by using controlled nozzle oscillation, *Key Eng Mater*, Volume 404, Pages33–44, (2009), doi: 10.4028/www.scientific.net/KEM.404.33.
 58. Deepak D, Anjaiah D, Shetty S, Optimization of process parameters in abrasive water jet drilling of D2 steel to produce minimum surface roughness using Taguchi approach, 6th International Conference on Electronics,

-
- Computer and Manufacturing Engineering, Pages 236–9, (2017), doi: 10.17758/EAP.U0317104.
59. K. Ravi Kumar, V.S. Sreebalaji, T. Pridhar, Characterization and Optimization of Abrasive Water Jet Machining Parameters of Aluminium /Tungsten Carbide Composites, Measurement, (2017), doi: 10.1016/j.measurement.2017.11.059.
60. Yuvaraj Natarajan, Pradeep Kumar Murugesan, Mugilvalavan Mohan, Shakeel Ahmed Liyakath Ali Khan, Abrasive Water Jet Machining process: A state of art of review, Journal of Manufacturing Processes, Volume 49, Pages 271-322, (2020), doi: 10.1016/j.jmapro.2019.11.030.
61. Jagadish, Gupta K., Introduction to abrasive water jet machining in abrasive water jet machining of engineering materials, Springer briefs in applied sciences and technology, Springer, Cham., Pages 1-11, (2020), https://doi.org/10.1007/978-3-030-36001-6_1.